TOPICAL REVIEW — Magnetism, magnetic materials and interdisciplinary research

Oxide magnetic semiconductors: Materials, properties, and devices

Tian Yu-Feng(田玉峰), Hu Shu-Jun(胡树军), Yan Shi-Shen(颜世申)†, and Mei Liang-Mo(梅良模)

School of Physics, Shandong University, Jinan 250100, *China*

(Received 29 April 2013)

We give a brief introduction to the oxide (ZnO, TiO_2, In_2O_3, SnO_2, etc.)-based magnetic semiconductors from fundamental material aspects through fascinating magnetic, transport, and optical properties, particularly at room temperature, to promising device applications. The origin of the observed ferromagnetism is also discussed, with a special focus on first-principles investigations of the exchange interactions between transition metal dopants in oxide-based magnetic semiconductors.

Keywords: magnetic semiconductors, ferromagnetism, spintronics, magnetic, transport, optical

PACS: 85.75−d, 75.50.Pp, 75.47.Lx, 75.70.−i **DOI:** 10.1088/1674-1056/22/8/088505

1. Introduction

The emerging research area termed "spintronics," which utilizes the spin degree of freedom in addition to the usual electron charge transport to realize functional devices, has developed quickly in recent decades.[1] Compared to conventional semiconductor devices, where only the charge of electrons is used, some predicted advantages of spintronics are increased speed of data processing, high data storage density, nonvolatility of data storage, and low energy consumption.[2] Current magnetic devices, such as read heads for magnetic data storage, are mainly based on ferromagnetic metals. The development of novel magnetic semiconductors compatible with modern industrial semiconductor growth techniques, would offer more possibilities to combine the semiconducting and magnetic properties.

In fact, pioneering studies of magnetic semiconductors in the 1960s showed the coexistence of semiconduction and magnetism in some ferromagnetic semiconductors, such as europium chalcogenides[3] and the spinel compounds $CdCr_2S_4$ and $CdCr_2Se_4$.[4,5] However, the low Curie temperature and poor reproducibility of these established magnetic semiconductors have limited their application. An alternative method is offered by the so-called diluted magnetic semiconductors (DMSs), where the coexistence of magnetism and semiconducting is achieved by doping magnetic atoms into nonmagnetic semiconductors.[6] II–VI compounds (such as CdTe, ZnSe, CdSe) doped with transition metal (TM) elements (such as Mn) became the most studied DMSs in the 1980s.[7,8] Though the presence of Mn in these alloys brings new physics by introducing localized spins, it cannot provide or trap carriers, i.e., n- or p-type doping cannot be achieved without additional dopants. Later on, the observation of hole mediated ferromagnetism (FM) in Mn-doped III–V group compounds, such as (In, Mn)As and (Ga, Mn)As, re-inspired the research interest in DMSs.[9–12] It is well accepted in Mn-doped III–V group DMSs that the long range ferromagnetic order between localized moments provided by substitutional Mn is mediated by the itinerate holes generated also by substitutional Mn through RKKY exchange coupling.[13] Owing to the strong coupling, novel phenomena, i.e., giant planar Hall effect[14] and anomalous Hall effect,[15] which are usually very weak or nonexistent in traditional non-magnetic semiconductors, have been observed. Great progress has been achieved, i.e., spin-involved devices based on GaMnAs, such as spin-polarized light emitters,[16] spin valves,[17] and spin field effect transistors,[18] have been demonstrated at low temperature. Unfortunately, though the Curie temperature of Mn-doped GaAs has been greatly improved compared to previous II–VI group compounds, it is still far below room temperature.[19–21] Besides the low Curie temperature of GaMnAs, another obstacle is the low mobility, which is physically limited by the large effective mass of holes.[22] Meanwhile, transition metal-doped elemental semiconductors (Si and Ge) showing ferromagnetic characteristics[23,24] have attracted extensive attention because of their compatibility with today's Si microelectronics. Recent advances here, as well as the challenges of moving TM-doped Group IV DMSs toward spintronics applications, have been discussed in several review papers.[25,26]

A milestone in the search for high Curie temperature DMSs is the theoretical prediction given by Dietl *et al.*,[13] that is, TM-doped (by Mn, etc.) wide band gap semiconductors (GaN and ZnO) exhibit ferromagnetism above room temperature when the hole concentration is on the order of

*Project supported by the National Natural Science Foundation of China (Grant Nos. 5125004 and 10974120), 111 Project (Grant No. B13029), and the National Basic Research Program of China (Grant Nos. 2013CB922303 and 2009CB929202).

†Corresponding author. E-mail: shishenyan@sdu.edu.cn

© 2013 Chinese Physical Society and IOP Publishing Ltd

10^{20} cm^{-3}. Soon after that, experimental room temperature ferromagnetism was reported in Co-doped TiO_2[27] and TM-doped ZnO.[28] These observations prompted extensive research work focusing on diluted magnetic oxide semiconductors (DMOSs), aiming to understand the mechanisms involved and to design better materials suitable for practical applications.

In the following, we would like to give a brief review focusing on recent advances as well as the imminent challenges in oxide magnetic semiconductors. First, various oxide candidates are summarized. Second, a brief description of sample synthesis and characterization methods is given, focusing on how to define intrinsic ferromagnetism. Third, the promising magnetic, transport, and optical properties of wide band gap oxide magnetic semiconductors are discussed in detail. Fourth, theoretical work focusing on the origin of ferromagnetism in oxide magnetic semiconductors is summarized. At last, attention is given to the principle oxide-based device applications, i.e., magnetic tunnel junctions, spin field effect transistors, etc.

2. Oxide candidates for magnetic semiconductors

Oxide materials have a long and magnificent research history. The first example of functional oxides are permanent magnets of lodestone consisting of Fe_3O_4 which were used as compasses in China, ancient Greece, and Sumer more than 2000 years ago.[29] In the 20-th century, ferromagnetic oxide nanoparticles (Fe_2O_3 and later CrO_2) have been utilized as recording media in magnetic tapes. Ferroelectric oxides were found later in history, with the first observation of electric hysteresis in Rochelle salt.[30] In 1986, a breakthrough was obtained for superconducting oxides — the discovery of superconductivity as high as 35 K in the La–Ba–Cu–O system.[31] Mixed valence manganites have been intensively explored because of their "colossal magnetoresistance" (CMR) and complex phase transitions.[32] It is now known that in CMR materials, rich physical properties are dominated by the "double exchange" interactions and Jahn–Teller distortions as a result of the complicated interactions between electronic, magnetic, and structural degrees of freedom. Half-metallic binary oxides such as Fe_3O_4, CrO_2, and EuO are also attractive candidates because of their high spin polarization ratio ($\sim$ 100%). In recent years, multiferroic oxides ($BiFeO_3$,[33,34] $BaTiO_3$,[35] $TbMnO_3$,[36,37] etc.) with more than two ferroic orders have become a fast developing research subject.

Most wide band gap materials are insulating, while most conducting materials are opaque to light at visible wavelengths. In this sense, wide band gap oxides semiconductors (ZnO, TiO_2, In_2O_3, etc.) are unique because they are good conductors due to the presence of native defects while simultaneously being transparent in the visible region.[38] Hence, among various promising oxide candidates for spintronics applications, wide band gap oxides based on diluted magnetic oxides, such as ZnO, TiO_2, In_2O_3, SnO_2, and $(In,Sn)_2O_3$ (ITO) doped with different transition metals (Co, Mn, Fe, Cu, Ni, V, etc.) and non-magnetic (N, H, etc.) dopants, attract the most attention. Furthermore, the magnetic properties of oxides span from diamagnetic, paramagnetic to ferromagnetic and antiferromagnetic, and their chemical reactivity can be tailored from being highly reactive to inert. All these promising properties originate from the strong and competitive exchange coupling between charge, orbital, lattice, and spin degrees of freedom in these oxide materials.[39]

As will be discussed later, one obstacle for the DMOSs is their weak magnetic signal as the doping concentration is usually only a few percent. One alternative solution is proposed by Yan *et al.*,[40,41] wherein concentrated oxide ferromagnetic semiconductors (COFSs) are prepared by alternately sputtering thin (less than 1 nm) ferromagnetic metal (Co, Fe) layers and oxide (ZnO, TiO_2, In_2O_3, etc.) layers. These COFSs with huge room temperature magnetization, large room temperature magnetoresistance, and giant room temperature magneto-optical Kerr rotation[42] are also promising candidates for future spintronics applications.

3. Sample preparations and characterizations

Benefits from the development of sample preparation techniques, high quality oxide thin films can be synthesized. Four kinds of techniques are usually utilized to grow crystalline oxide films: pulsed laser deposition (PLD), molecular beam epitaxy (MBE), magnetron sputtering, and chemical vapor deposition (CVD).[43] The physical mechanisms used to generate the gaseous beams are different from each other. For example, in PLD one uses high energy laser pulses to ablate a target and the resulting ions from the target can have energy as high as $\sim$ 100 eV. In contrast, in MBE growth, beams with low energy ($\sim$ 1 eV) are generated by thermal effects. In CVD growth, volatile molecular precursors are exposed to the heated substrate where precursor decomposition is driven by thermal energy. As a result of metal–organic precursor decomposition, H or C impurities may be introduced into the films. In magnetron sputtering growth, plasma is generated by applying a high voltage between a target and cathodes, ejecting (sputtering) ions from the target toward the substrate. Because of its high reproducibility and ability to obtain uniform films in large scale, sputtering is widely used in today's electronics industry.

After various reports on ferromagnetism in TM-doped DMOSs, where DMOSs refers to a non-magnetic semiconductor with a homogeneous distribution of a few-percent concen-

tration of magnetic dopants, it turns out that instead of preparation methods, FM is more sensitive to the detailed preparation conditions, i.e., substrates, temperature, oxygen partial pressure, and post annealing conditions. Before discussing the current research status of the oxide magnetic semiconductors, it is worth mentioning how to define intrinsic ferromagnetism in DMS materials. Because DMSs are usually synthesized by incorporating magnetic transition metal elements into nonmagnetic semiconductors, it is important to make sure that the observed ferromagnetism is not from magnetic clusters, contaminations or other artifact effects. In the following we would like to briefly introduce the experimental tools commonly used to investigate the DMOSs.

(i) X-ray diffraction (XRD). XRD, including rocking curve, pole figure, and reciprocal space mapping measurements, is a convenient technique to characterize the microstructures of materials. For example, in Ag-doped ZnO bulk samples, when the doping concentration reaches 8%, Ag impurity peaks are clearly revealed in the XRD results.[44] In $Zn_{0.95}Ni_{0.05}O$ films, Ni impurity peaks, which are absent in samples grown at high oxygen pressure (10^{-3} Torr, 1 Torr = 1.33322×10^2 Pa), have been observed in the samples prepared in low oxygen pressure (10^{-6} Torr).[45] However, when the doping concentration is low or the impurity clusters are quite small, it is beyond the detection limit of XRD.[46]

(ii) Transmission electron microscopy (TEM). TEM utilizes energetic electrons to provide morphologic, crystallographic, and compositional information about the studied samples. High resolution TEM (HRTEM), has become one of the most powerful tools in microstructure characterization, because of its ability to show lattice information in a length scale less than 0.5 nm. For example, in $Ti_{0.98}Co_{0.02}O_{2-\delta}$ films, Co nanoparticles with a diameter of $\sim$ 10 nm, located at the interface between film and substrate, have been directly observed by TEM studies.[47] In Co-doped ZnO prepared by the sol–gel coating method, Co clusters, also directly found via the HRTEM, were responsible for the observed ferromagnetism.[48] However, because the TEM usually only shows the detailed structure information of a tiny partial area, it cannot effectively present macroscopic information.

(iii) Electron energy loss spectroscopy (EELS) and X-ray photoelectron spectroscopy (XPS). The substitution of TM elements in DMOSs can be elucidated by means of EELS and XPS, where the valence states of the TM dopants can be obtained. For example, in Mn-doped ZnO, the shoulder presented in the nearedge structure of O–K and the Mn–L_3/L_2 intensity ratio from the EELS spectra indicates Mn to be in the +2 valence state.[49] In Co-doped ZnO, XPS has been used to characterize the charge state of the Co ions, where from the Co 2p core level photoemission spectrum, Co was found to be in the +2 oxidation state as long as the concentration of Co is less than 35%.[50,51]

(iv) X-ray absorption spectroscopy (XAS). XAS is another useful tool to elucidate the formal charge state and the local structural environment surrounding the TM dopants. For instance, studies have been performed on the TM K-edge, TM L-edge, and O K-edge.[52,53] Its potential to provide local chemical information and its high sensitivity to the subtle difference in local arrangement have drawn increasing attention.[54,55]

(v) Electron spin resonance[56] and Mössbauer spectroscopy[57] have also been used to investigate the local magnetic structures. On the other hand, by measuring the optical properties, using Raman spectroscopy[58,59] and optical transmittance (absorption) spectroscopy,[60,61] the valence state of the transition metal dopants in DMOSs can be illustrated.

(vi) Magnetic circular dichroism (MCD). MCD, which is sensitive to magnetism in specific elements, is considered to be one of the most powerful tools to identify the existence of intrinsic ferromagnetism. The appearance of MCD is directly connected to the spin polarization of a semiconductor band, which is due to the quantum mechanical selection rules for optical absorption. All magnetic materials produce an MCD signal, but for intrinsic DMSs or DMOSs, not only a strong MCD signal is expected, but also an MCD spectral shape that reflects the band structure of the host semiconductors should be exhibited[62–64] (as shown in Fig. 1). MCD has been widely used as important evidence for the existence of intrinsic ferromagnetism in TM-doped ZnO DMOSs.[63,64]

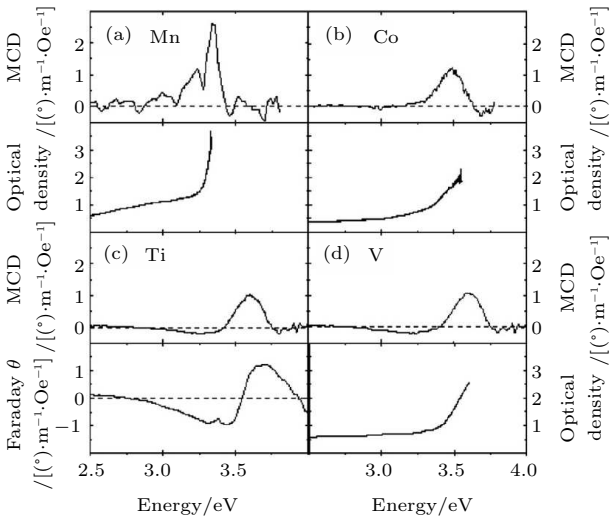


Fig. 1. Room temperature MCD measurements of ZnO doped with (a) Mn (2%), (b) Co (2%), (c) Ti (2%), and (d) V (5%). The optical absorption data for the Mn-, Co-, and V-doped samples and the Faraday rotation data for the corresponding Ti-doped samples are also shown. Reprinted with permission from Ref. [63]. The unit 1 Oe = 79.5775 A·m^{-1}. Copyright (2006) by the American Physical Society.

(vii) Magnetic zero field cooling (ZFC) and field cooling (FC) curves. Through systematic analysis of the ZFC–

FC magnetic behaviors, it is possible to investigate the existence of magnetic nanoclusters.[65,66] For instance, Martínez *et al.*[66] reported that in Co-doped ZnO nanoparticles, although XRD and high resolution electron microscopy show the absence of any Co segregation or any phase other than würtzite ZnO, ZFC–FC magnetization curves show the typical behavior of an assembly of superparamagnetic nanoclusters with irreversibility between the ZFC and FC branches below the blocking temperature (as shown in Fig. 2).

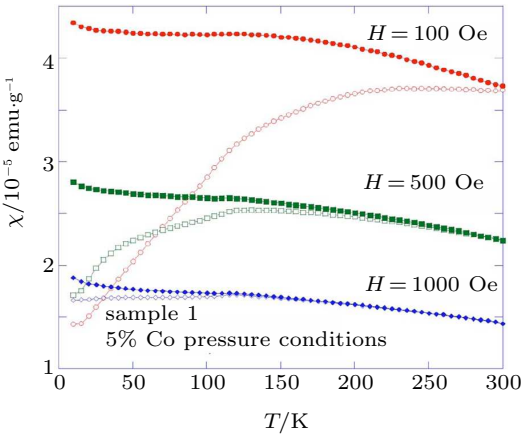


Fig. 2. Thermal dependence of the magnetic susceptibility of $Zn_{0.95}Co_{0.05}O$ sample after a ZFC–FC process. Reprinted with permission from Ref. [66]. Copyright (2006) by the American Physical Society.

(viii) Anomalous Hall effect (AHE). AHE occurs in materials with broken time-reversal symmetry, typically in ferromagnetic materials, as a result of spin-orbital coupling.[67] Hence, it is directly related to the exchange coupling between localized magnetic and itinerate carriers. In addition, AHE is insensitive to magnetic contaminations and other artificial effects, compared to magnetic measurements. As a result, AHE has also been considered as a useful tool to determine whether TM-doped DMOSs, such as Co-doped ZnO[68–70] and Co-doped TiO_2,[71] are intrinsic DMSs or not. For highly insulating magnetic oxide samples where conventional transport measurements cannot be performed, ferroelectric testing and impedance spectroscopy have been utilized to identify the relationship between magnetization and the carriers.[55]

Moreover, because carriers play a crucial role in mediating the exchange coupling, any independent manipulation of carrier density, for instance, by external electrical field in a field effect transistor or by co-doping, should have a direct influence on the ferromagnetism. Although the phenomena of MCD, AHE, and electric field modulation of ferromagnetism can be regarded together as the signature of intrinsic ferromagnetism, caution needs to be exercised before arriving at a definitive conclusion of the observation of intrinsic ferromagnetism, because the above-mentioned effects can appear in cases where the dopant distribution is inhomogeneous and/or the dopants are partially clustered.

4. Fascinating properties of oxide ferromagnetic semiconductors

Extensive efforts are devoted to the development of oxide ferromagnetic semiconductors suitable for spintronics applications, because of the prospects of achieving new functionality via controlled modification of magnetic, electronic, and photochemical properties. The first step toward magnetic property modification is searching materials with reproducible and stable room temperature ferromagnetism. In the case of electronic modifications, conductivities of semiconducting oxides can be changed by several orders of magnitude by doping. For example, doping $SrTiO_3$ (STO) with a few parts per thousand of Nb changes the transparent STO into dark gray, strongly n-type semiconductors. Combining the spin degree of freedom of oxide ferromagnetic semiconductors, it is possible to manipulate the transport behavior of the spin polarized carriers by applying magnetic fields. While in the photochemical area, not only is magnetic doping an effective method to shift the band gap of oxide photocatalysts such as TiO_2 from the visible into the UV range, but it also facilitates novel photochemical reactions differing from the host materials by introducing impurity bands. In the following, we would like to give a brief summary of the current research status of the wide band gap oxide ferromagnetic semiconductors, including the magnetic, electrical transport, and optical properties.

4.1. Magnetic properties

4.1.1. TM-doped diluted magnetic oxide semiconductors

In the search for intrinsic high Curie temperature magnetic semiconductors, ZnO-, TiO_2-, In_2O_3-, and SnO_2-based wide band gap oxide semiconductors are among the most extensively explored materials, including 3d TM-doped materials, co-doped materials, non-magnetic element-doped materials, and undoped materials, because of both the hope generated by early research and additional application-worthy properties revealed more recently.[72–75] In the following we would like to discuss the research on several wide band gap oxide material systems that have been central in the DMOS research.

4.1.1.1. ZnO-based magnetic semiconductors

ZnO is one of the most investigated oxides due to its unique physical properties. The stable crystal structure of ZnO is wurtzite with a direct bandgap of 3.4 eV. It has a shallow donor level due to the existence of native defects, such as oxygen vacancies and Zn interstitials, and a very high electron mobility of 200 $cm^2/V{\cdot}s$. The wide band gap in combination with high conductivity holds promise for applications in surface acoustic wave devices and transparent conducting electrodes. Since the valence of Zn is 2+, which can be adopted by many 3d TM ions, incorporating TM ions substitutionally

into ZnO is relatively easy and a higher doping concentration can be achieved.

The first investigation of ferromagnetism in 3d TM-doped ZnO films was performed by Ueda *et al.*,[28] wherein some ferromagnetic features were observed only in $Zn_{1-x}Co_xO$ rather than in Cr-, Ni- or Mn-doped films. Later, various 3d TM elements, such as Sc,[76–78] Ti,[76–78] V,[77,78] Fe,[79,80] Co,[28,81] Ni,[82,83] Cr,[84–86] Mn,[49,87–89] Cu[90–94] have been extensively explored. For instance, room temperature FM is observed in ZnO films synthesized using targets containing 5 at% of Sc, Ti, V, Fe, Co, and Ni, but not Cr, Mn, and Cu ions, as is shown in Fig. 3.[77,78] It is clear that the observed ferromagnetism is very anisotropic, with the largest moment 2.6 μ_B/dopant atom for a Co-doped sample under parallel magnetic field.[78] In addition, with increasing Co concentration, the moment/Co decreases as a result of the increasing Co–Co antiferromagnetic coupling between neighboring dopants.[78] The first observation of room temperature FM in diluted Mn-doped ZnO was reported by Sharma *et al.*,[49] where an average magnetic moment of ~ 0.16 μ_B was obtained. More detailed work on low temperature processed Mn-doped ZnO was performed by Ogale and co-workers,[87] wherein they demonstrated that room temperature FM in Mn-doped ZnO does not originate from carrier induced exchange coupling between Mn dopants, but rather comes from a new metastable ferromagnetic phase.

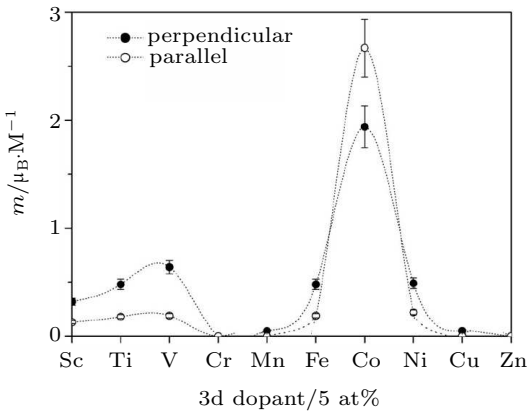


Fig. 3. Magnetic moment of 3d TM-doped ZnO films measured at room temperature under both parallel (open circles) and perpendicular (solid circles) applied magnetic field. Reprinted with permission from Ref. [78]. Copyright (2004) by the American Physical Society.

Furthermore, the observed ferromagnetism could be manipulated by both physical and chemical treatment. Schwartz and Gamelin[95] reported that in Co^{2+}:ZnO the room temperature (RT) ferromagnetic ordering could be switched back and forth reproducibly by introducing and removing native interstitial Zn as shown in Fig. 4, where a double-exchange mechanism for ferromagnetism involving electron delocalization on Co ions was proposed. Kittilstved *et al.*[96] demonstrated that ferromagnetism in Co^{2+}:ZnO and Mn^{2+}:ZnO can be modified in predictable and reproducible ways by using targeted n- and p-type chemical perturbations as shown in Fig. 5. These data are not only consistent with the prediction from carrier-mediated ferromagnetism, but also suggest that it may eventually be possible to use *ex situ* chemical, physical or even optical perturbations to manipulate the magnetic ordering in DMOSs.

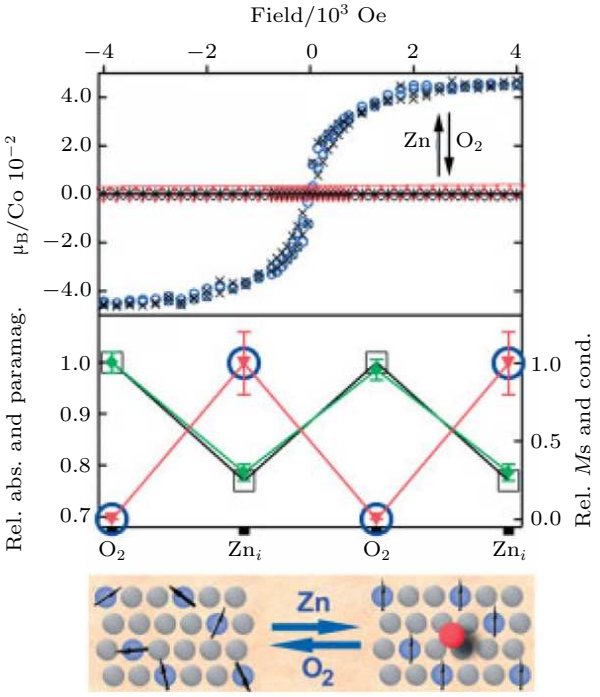


Fig. 4. (a) Reversible room temperature ferromagnetism for the 3.61% Co:ZnO thin films, using alternating Zn_i incorporation and oxidation with O_2 (sequence: × (O_2), ◯ (Zn_i), □ (O_2), + (Zn_i)). (b) The correlated switching of the 300-K $^4A_2 \rightarrow {}^4T_1$(P) ligand-field absorption intensity (black), 10-K Co paramagnetism (green), 300-K saturation magnetic moment (blue), and conductivity (red) for the above sample. (c) Schematic illustration of the effect of Zn_i on the ferromagnetic ordering. Reprinted with permission from Ref. [95]. Copyright (2004) by the WILEY-VCH Verlag GmbH & Co. KGaA, Weinheim.

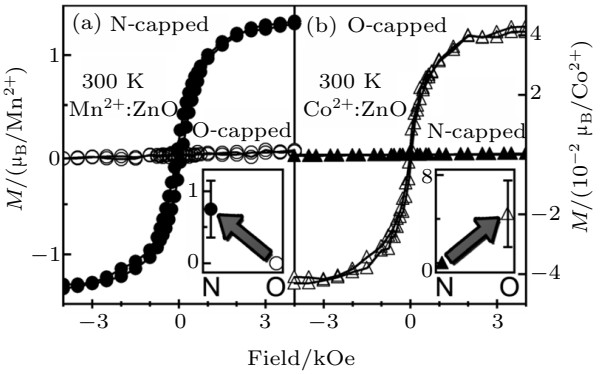


Fig. 5. Room temperature hysteresis loops for (a) 0.20% Mn^{2+}:ZnO and (b) 3.5% Co^{2+}:ZnO films prepared from N-capped (solid) or O-capped (hollow) colloids. Insets: statistics for room temperature ferromagnetic saturation moments obtained from ≥10 independent films for each case. Reprinted with permission from Ref. [96]. Copyright (2005) by the American Physical Society.

In an ideal case, doping Co or Mn into ZnO should only

introduce local magnetic moments without introducing additional carriers, since the valence state of Zn is 2+, which is the same as that of the substitutional Co or Mn dopant. Hence, this system could allow more direct exploration of the question of whether the observed room temperature FM is carrier-mediated or not. Accordingly, some studies have been performed on the properties of TM-doped ZnO in which an electronic dopant such as Al was deliberately doped to tune the carrier concentration.[97–99] For example, Behan *et al.*[99] studied the magnetic properties of (Co, Al) and (Mn, Al) co-doped ZnO with a very wide range of carrier densities (from 10^{17} cm^{-3} to 10^{21} cm^{-3}). As shown in Fig. 6, robust room temperature FM was observed both in the insulating regime with a carrier concentration of 10^{17} cm^{-3} $\sim$ 10^{18} cm^{-3} range and the metallic regime with a carrier concentration around 10^{20} cm^{-3}. However, ferromagnetism is quenched when carrier concentration was in an intermediate regime. It was proposed that variable range hopping (VRH) combined with magnetic polaron formation is responsible for the room temperature FM in the insulating regime, while standard carrier-mediated room temperature FM is dominant in the metallic regime. The absence of room temperature FM in the intermediate carrier range was explained as a result of the spin flip caused by a sudden polaronic density change near Co due to the hopping of a mobile carrier.[99]

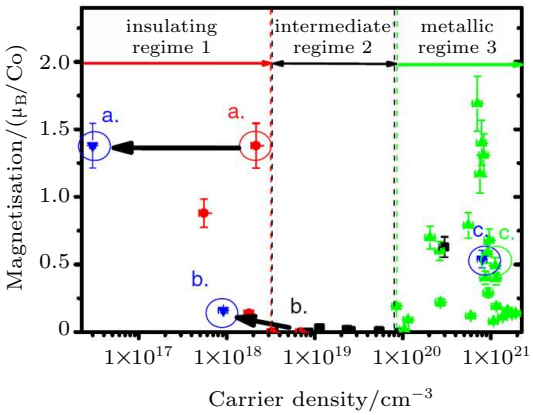


Fig. 6. Room temperature magnetization for (Co,Al) co-doped ZnO films as a function of the mobile carrier density. Reprinted with permission from Ref. [99]. Copyright (2008) by the American Physical Society.

However, different conclusions have been obtained. That is, structurally excellent crystalline films of Mn- and Co-doped ZnO are paramagnetic, even in the presence of sufficient itinerant carriers,[48,76,89,100–102] which makes the observed room temperature FM controversial. Using synchrotron radiation, Ney *et al.*[101] performed element-specific structural and magnetic investigations on the $Zn_{1-x}Co_xO$ epitaxial system. It was found that although Co dopants exclusively occupy Zn sites, purely paramagnetic behavior is observed for isolated Co dopants, and Co–O–Co pairs are antiferromagnetically coupled. Kaspar *et al.*[102] investigated the magnetic properties of Co-doped ZnO with high structural quality and a wide range of conductivities (10^{-4} Ω·m–10^{5} Ω·m), which was achieved by controlling deposition oxygen pressure, post annealing conditions, and/or Al co-doping during deposition. In no case were ferromagnetic signatures observed, indicating that itinerant conduction band electrons alone are insufficient to induce room temperature FM. Further in-depth investigation leads to the suspicion that the combination of Co and point defects are responsible for the appearance of room temperature FM. Point defects could mediate effective exchange coupling between Co spins via bound magnetic polaron formation. Also it has been suggested that defects at small-angle grain boundaries in epitaxial films could be the source of polaronic carriers.[43] Unfortunately, these defects are extremely difficult to detect experimentally.

4.1.1.2. TiO_2-based magnetic semiconductors

Since the first report of DMOSs ferromagnetism in Co-doped TiO_2,[27] TiO_2-based DMOSs become the most explored oxide systems.[72,74] TiO_2 has three basic polymorphs, i.e., rutile, anatase, and brookite. Rutile is tetragonal (a = 4.59 Å and c = 2.96 Å) with an indirect bandgap of 3 eV, which is considered to be the most stable configuration and can be grown using $LaAlO_3$ (001), $SrTiO_3$ (001) substrates, while the anatase phase also crystallizes in a tetragonal structure (a = 3.78 Å and c = 9.52 Å) with a bandgap of 3.2 eV, which is promising for photo–electro–chemical use, and it can be grown on Si (100), Al_2O_3 (001) substrates.[73,75] In a pioneering study performed by Matsumoto *et al.*,[27] room temperature FM with a magnetic moment $\sim$ 0.32 μ_B/Co was achieved, wherein the Co ions were believed to be in the low spin configuration. Later, the reported room temperature magnetic moments in $Ti_{1-x}Co_xO_2$ vary from $\sim$ 0.16 μ_B/Co[103] to $\sim$ 1.7 μ_B/Co,[104,105] and even exceed the moments of Co metal (1.76 μ_B/Co).[106]

In order to elucidate whether the observed ferromagnetism is intrinsic or not, multiple methods have been utilized, such as XPS, XAS, MCD, AHE, etc. The charge state of Co in TiO_2 has been determined to be +2 by using both XPS and XAS,[72] but further investigations are needed to determine whether the ionic ground state of Co^{2+} is the high spin ($3d^7$ $S = 3/2$)[105] or low spin state ($3d^7$ $S = 1/2$).[107] Yamada *et al.*[108] performed a systematic study of the structures, electronic, and magneto–optical properties of anatase phase Co-doped TiO_2. Not only is a large MCD signal observed at a photon energy close to the band gap of TiO_2, but the intensity of the MCD signal increases with both the increase of carrier density and doping concentration. These data demonstrate that interaction between carriers and Co impurities is essential to the room temperature FM in the $Ti_{1-x}Co_xO_2$ (x = 0–0.10) system. Soft X-ray magnetic circular dichroism (XMCD) measurements were performed on Rutile $Ti_{1-x}Co_xO$ by Mamiya *et*

al.,[109] revealing that room temperature FM originates from Co^{2+} ions substituting for Ti^{4+}ions. In addition, the connection between carrier density and ferromagnetism has been indicated by the AHE in Co-doped TiO_2.[110–113] For example, Toyosaki *et al.*[110] reported finding AHE in rutile phase $Ti_{1-x}Co_xO_2$ grown by laser molecular beam epitaxy, supporting the belief that the carrier-mediated room temperature FM is intrinsic. Ueno *et al.*[111] reported finding AHE in anatase $Ti_{1-x}Co_xO_2$, where the magnetic field dependence of AHE coincides with that of magnetization. Toyosaki *et al.*[112] and Fukumura *et al.*[113] studied the magnetic properties of rutile $Ti_{1-x}Co_xO$ using MCD, AHE, and magnetic measurements as well. They found that the observed magnetization depends on both carrier concentration and doping concentration. Moreover, the magnetic field dependence of the MCD signal shows good coincidence with those of both magnetization and AHE, strongly suggesting that carrier induced intrinsic ferromagnetism can occur in this system. Similar conclusions have been obtained by other groups.[114–116] It is worth mentioning that Shinde *et al.*[47] performed a detailed magnetic and structural analysis of highly reduced rutile $Ti_{1-x}Co_xO_2$. The cusp feature in ZFC–FC curves suggests the presence of nanoparticles, which has been directly confirmed by using TEM. Surprisingly, AHE is clearly observed. The co-occurrence of superparamagnetism and AHE raises a question regarding the use of AHE as definitive evidence for the existence of intrinsic ferromagnetism.

Beside Co, other TM elements, such as Fe,[117,118] Cr,[118–120] V,[118] Ni,[118] etc., have also been doped into TiO_2. For example, Cr-doped TiO_2 draws increasing attention, as Cr dopant seems to have no tendency to segregate and/or precipitate into different phases up to a Cr concentration as high as 16 at%. Wang *et al.*[121] reported a hole mediated, RKKY-like interaction-induced high temperature ($T_c \geq 400$ K) ferromagnetism in rutile $Ti_{1-x}Cr_xO_2$ with a saturation magnetic moment 2.9 μ_B/Cr for $x = 0.06$ and 0.9 μ_B/Cr for $x = 0.12$, respectively. In contrast, Droubay *et al.*[122] found room temperature FM in insulating anatase Cr-doped TiO_2 with a saturation magnetization of ~ 0.6 μ_B/Cr. This indicates that rather than itinerate carrier-mediated ferromagnetism, F-center exchange-induced bound magnetic polarons are responsible for the observed ferromagnetism in the insulating case. Moreover, Kaspar *et al.*[119] reported that ferromagnetism can be obtained only in structurally defective $Ti_{1-x}Cr_xO_2$, while negligible magnetism is found in $Ti_{1-x}Cr_xO_2$ that is of excellent structural quality, which indicates that charge-compensating oxygen vacancies alone are not sufficient to induce ferromagnetism, contrary to the prediction of the F-center model. Hence, the mechanism of ferromagnetic interaction could be quite different, even for the same system, and needs further investigations.

4.1.1.3. SnO_2-based magnetic semiconductors

Inspired by the research into TiO_2-based DMOSs, some researchers have looked at another rutile-type material, i.e., SnO_2. So far, magnetic properties of Co-,[123,124] Mn-,[124,125] Fe-,[124,126] Cr-,[69] Ni-,[69,127] Cu-,[128] etc., doped SnO_2 have been studied. Interesting work by Ogale *et al.*[123] with Co-doped SnO_2 showed that ferromagnetism up to 650 K can be obtained for $Sn_{0.95}Co_{0.05}O_2$. More importantly, a giant magnetic moment of $(7.5 \pm 0.5$ μ_B/Co was discovered for the first time in DMOSs. Later, giant magnetic moments were also confirmed in TM-doped ZnO[51,129] and TM-doped SnO_2.[69] The giant magnetic moments in Co:SnO_2 have been attributed either to atoms surrounding the Co atoms, which acquired moments through electronic effects, or to the orbital moments of Co remaining unquenched for some unknown reasons.[123] Nevertheless, the state giving giant magnetic moments is possibly a highly unstable state, which is usually observed in the diluted doping condition and can be eliminated by both post annealing and increasing doping concentration.[69] The origin of such a giant magnetic moment is still an open issue.

4.1.1.4. In_2O_3-based magnetic semiconductors

In_2O_3 is a well-known transparent oxide semiconductor that can be made highly conductive by introducing oxygen vacancies or Sn doping, so ferromagnetic In_2O_3 materials are attractive candidates for magneto–optical and spintronics devices. Room temperature FM has been observed in Fe-,[130–132] Co-,[133] Ni-,[134] Cr-,[135–137] V-[138] doped samples as well codoped samples.[139,140] For instance, through extensive studies microstructure, composition, and magnetic properties, Xing *et al.*[132] found that Curie temperature in Fe-doped In_2O_3 can be as high as 927 K with a strong perpendicular magnetic anisotropy and a coercivity of 680 Oe at room temperature.

4.1.1.5. Cu_2O-based magnetic semiconductors

Cu_2O is another interesting candidate because it is a p-type semiconducting oxide. Kale *et al.*[141] first made a series of films of 5% Co-doped Cu_2O without and with 0.5% codoping with Al, V, or Zn. Spin glass behavior was found in samples without co-doping, while room temperature FM was observed for Co, Al co-doped films with a saturation moment of 0.44 μ_B/Co. The authors suspected that an orbital defect state may be involved in producing the room temperature FM. Also, based on the Co:Cu_2O system, Raebiger *et al.*[142] proposed a new model for the appearance of ferromagnetism, wherein the occupation of the previously unoccupied states when two TM impurities form a close pair plays the critical role. Other host oxide materials have also been used to search for DMOSs, such as $La_{1-x}Sr_xTiO_3$, $KTaO_3$, Fe_3O_4, etc. The recent progress has been summarized by several review papers.[43,74,75]

4.1.2. d^0 ferromagnetism

There are a relatively large number of reports of unexpected weak ferromagnetism in the "d^0 systems," in which there are no magnetic dopants.[143] The discussion was triggered by the observation of ferromagnetism in HfO_2 with a moment of ~ 0.15 μ_B per HfO_2 formula unit and a giant anisotropy,[144,145] which depends on both the substrate and film texture. And later, d^0 ferromagnetism was demonstrated in undoped TiO_2,[146] ZnO,[147,148] In_2O_3,[146,149] SnO_2,[150] Al_2O_3,[147] etc., and Sc-, Ti-, and C-doped ZnO as well.[151] As there are usually no known ferromagnetic secondary phases of Zn, Sc, or HfO_2, secondary ferromagnetic phases cannot be a general and convincing explanation. A common feature is the presence of lattice defects, since none of the above mentioned materials are ferromagnetic in bulk when they are defect-free. Several plausible models have been proposed. For example, defects in a semiconductor or insulator could create states in the bandgap, if the density of states is sufficiently large, spontaneous spin splitting may emerge based on the Stoner criterion. On the other hand, it is also believed that defect states themselves could give rise to magnetic moments by involving the molecular orbital localized in the vicinity of the defects to form an impurity band that is necessary to mediate a long range magnetic coupling.[143] Recently, a new model was developed for defect-related ferromagnetism for DMOSs, involving a spin-split defect impurity band populated by charge transfer from a proximate charge reservoir.[152] In oxides, defect states are typically oxygen vacancies and/or metal interstitials.[143] It is worth mentioning that the formed impurity band does not have to be conducting. As long as the localization length is larger than the distance between localized moments, ferromagnetism could be established. So far, the origin of observed magnetization anisotropy in these films remains an open question, and needs further in-depth theoretical investigations.

4.1.3. Magnetic properties of concentrated oxide ferromagnetic semiconductors

The moments of a typical DMOS sample are of the order 10^{-8} A·m^2 or even less, which is near the limit of sensitivity of instruments used to characterize magnetic properties, such as VSM (10^{-9} A·m^2). As a result, the hidden secondary phases, contamination, measurement artifacts could provide comparable magnetic signals.[153,154] An alternate material with suitable magnetic moments for practical applications is the concentrated oxide ferromagnetic semiconductors (COFSs). As mentioned previously, amorphous or nanocrystal COFSs with high TM concentration can be synthesized by alternatively sputtering very thin TM and oxides layers under thermal non-equilibrium conditions. In such a way, Co:ZnO,[40,155] Fe:ZnO,[156,157] Co:TiO_2,[41] Co:Al_2O_3,[158] and Fe:In_2O_3[159] COFSs have been successfully synthesized. The magnetization at room temperature can be as high as $\sim$ 580 emu/cm^3 (~ 0.78 μ_B/Co) for Co:ZnO and $\sim$ 500 emu/cm^3 (~ 1.24 μ_B/Co) for Co:TiO_2.[40,41] In these special systems, many defects, such as O vacancies and TM interstitials, can exist and provide s, p carriers, which lead to the spin–spin exchange interaction between s, p carriers and localized d electrons of doped TM elements. There also exist direct d–d exchange interactions between neighboring TM dopants as a result of high TM concentration. Therefore, localized TM dopants can establish local ferromagnetic structures and even long range ferromagnetic ordering through either s, p–d or d–d exchange coupling between neighboring TM dopants.

4.2. Transport properties

To move toward utilizing and manipulating the spin degrees of freedom, it becomes crucial to understand the behavior of the spin polarized carrier inside both ferromagnetic oxide semiconductor materials and artificially constructed devices. In the following we would like to give a brief summary of the most extensively studied transport behaviors of ferromagnetic oxide semiconductors, i.e., magnetoresistance and the anomalous Hall effect.

4.2.1. Magnetoresistance

Magnetoresistance (MR) represents the change in resistance with applied magnetic field and hence demonstrates the interaction between free carriers and localized magnetic moments. The study of MR in ferromagnetic materials started as early as 1857 with the measurement of anisotropic MR in Ni and Fe. Recently, extensive effort has been applied to the magnetotransport phenomena in oxide magnetic semiconductors, motivated by the rapid increase of data storage density in magnetic storage devices where magnetoresistive read-out technique is employed in the read heads. Unfortunately, the reported magnetotransport behavior in DMOSs is quite controversial since not only negative MR but also positive MR or a combination of the two have been observed.[160–163] The variety of MR in magnetic oxide semiconductors reflects the competing mechanisms dominating different fields as a result of the complex couplings between the spin, orbital, spin–spin, and spin–orbital interactions.

The positive MR in ZnO-, TiO_2-, and In_2O_3-based DMOSs is commonly attributed to the quantum correction on the conductivity due to the influence of the s–d exchange coupling-induced spin-splitting on the spin disorder-modified electron–electron interactions.[161,164–167] On the other hand, the negative MR, especially at low magnetic field, is usually attributed to the destructive effect of the weak

localization.[160,165] Weak localization is quantum-mechanical in nature and is a result of the diffusive motion of electrons in a highly disordered electronic system. The effect manifests itself as a positive correction to the resistivity. Systems with $k_F l > 1$ will be in the weakly localized regime, where k_F is the Fermi wave vector and l is the carrier mean free path. In line with the weak localized effect, negative MR has also been widely attributed to the decreased spin-dependent scattering as a result of the formation of magnetic polaron.[164,168,169] However, different mechanisms have also been reported. For instance, negative MR has been attributed to the spin-dependent hopping or magnetic field-induced variation of the Anderson localization length,[170] and to the high-order expansion of the s–d exchange coupling.[171,172] Giant positive MR with the temperature dependence $\ln(R_{(H)}/R_{(0)}) \sim T^{-1}$ in Co-doped ZnO nanocluster films is believed to be a result of the suppression of spin-dependent hopping when localized states with onsite correlation undergo large Zeeman splitting.[173,174] Besides spin-related effects, positive MR found in oxide ferromagnetic semiconductors has been attributed to purely orbital effects, which is not expected in the sense of manipulating spin polarized carrier transport. For example, positive MR could arise from the action of the Lorentz force on the mobile carriers.[175] For carriers in closed orbits, this positive MR is quadratic in low magnetic field and saturates in high magnetic field. While for carriers in open orbits, due to the reduced sample dimensions, this positive MR is quadratic and non-saturating. In the VRH regime, especially at sufficiently low temperatures where carrier hopping distance is relatively large, a large positive MR could originate from a sharp decrease in the overlap of wave-function "tails" between different states, i.e., wave-function shrinkage effect.[176,177]

It should be pointed out that the above-mentioned MR behavior of DMOSs was usually observed at low temperature and vanished at room temperature. Compared to DMOSs, COFSs could provide a much larger negative MR, 11% negative MR at room temperature.[40] In these COFSs, the dominant transport mechanism at low temperature regime is the thermal assisted spin-dependent VRH, while at high temperature, nearest neighbor hopping and/or direct tunneling can also contribute to the conductivity. By considering spin–spin exchange interactions ($E_{ex} = -(J/r)\cos\theta$), electron–electron Coulomb interaction ($E_{Co} = e^2/\varepsilon r$) and the "hard gap" energy simultaneously, the spin-dependent VRH model is proposed.[157,159,178] Here, J/r is the effective exchange coupling coefficient between two carriers, θ is the angle between the spin in the initial and final states, ε is the effective dielectric constant. Not only good agreement between theoretical predication and experimental observation was achieved (as shown in Fig. 7), but also a convenient method to estimate the spin polarization ratio of an oxide ferromagnetic semiconductors was provided. The spin polarization ratio of the $Zn_{0.28}Co_{0.72}O$, $Ti_{0.24}Co_{0.76}O_2$, $Zn_{0.14}Fe_{0.86}O$ is estimated to be $P = 29.6\%$, $P = 21.9\%$, and $P = 30.0\%$, respectively.[157,178]

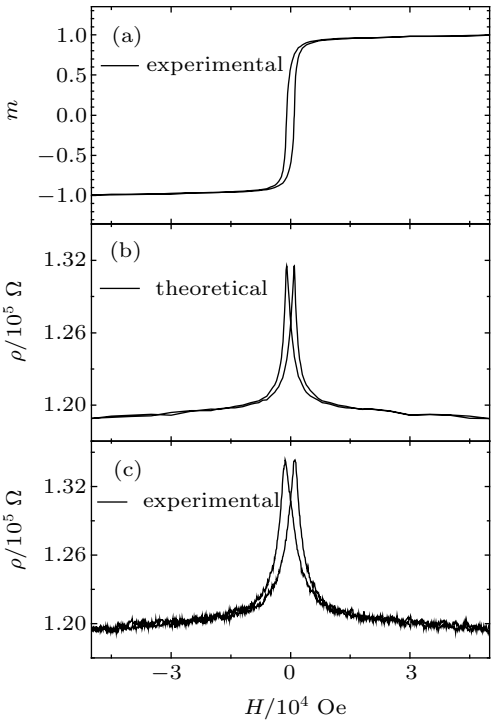


Fig. 7. Direct comparison among the experimental m–H curve (a), the theoretical (b), and experimental (c) ρ–H curves measured at 5 K for $Ti_{0.24}Co_{0.76}O$ COFS film. Reprinted with permission from Ref. [178]. Copyright (2006) by the IOP Publishing Ltd.

Anisotropic MR (AMR), which depends on the square of the spin–orbital coupling, is an important but seldom studied magnetotransport behavior. Previous studies from different groups contradict each other. Some researchers have shown that MR is independent of the orientation of the applied field with respect to the current and/or the crystalline axis, while others have demonstrated that MR is sensitively dependent on the field direction and/or the crystalline axis.[97,162,169,179,180] Because the carriers are usually s electrons in oxide ferromagnetic semiconductors,[97,162,180] the effect of spin–orbital coupling are rather smaller compared with p-type $Ga_{1-x}Mn_xAs$ DMSs where carriers are holes with much larger effective mass.[181] For example, Tian *et al.*[180] performed a systematic study of the anisotropic MR of Cu-doped ZnO with different crystalline orientations. Their comparative data of angular-dependent MR show that out-of-plane AMR comes from the geometric effect, while in-plane AMR results from the field-dependent path-length effect. As shown in Fig. 8, the small magnitude of AMR and the negligible magnetocrystalline anisotropy reflects the weak spin–orbital coupling in TM-doped ZnO systems.[180]

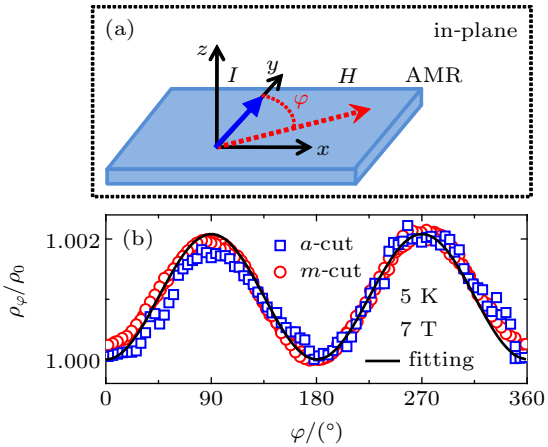


Fig. 8. (a) Schematic plot of the experimental configuration for the in-plane AMR measurement. (b) In-plane MR, ρ_φ/ρ_0, for the Cu-doped ZnO films grown on two different sapphire substrates. Reprinted with permission from Ref. [180]. Copyright (2012) by the American Institute of Physics.

4.2.2. Anomalous Hall effect

It is well known that the ordinary Hall effect is a result of the Lorentz force acting on the charges of moving carriers, while the anomalous Hall effect is highly sensitive to magnetization, that is, the spin degree of carriers. In addition, AHE is not affected by small amounts of segregation. Hence, it is a good measure of ferromagnetism for DMOSs. As a result, AHE has been widely used as a useful tool to distinguish the existence of intrinsic FM in Co-doped TiO_2,[47,71,111–113,115,116,182] Co- or Ni-doped ZnO,[45,68] Co-doped SnO_2,[69] FeCu-doped In_2O_3,[183] and Mn-doped ITO, etc.[70] For example, in Co-doped TiO_2, the AHE together with magnetization, magnetic circular dichroism measurements have been examined for samples with various electron concentrations.[113] The sample with high electron density shows the same magnetic field dependence for AHE, MCD, and magnetization (as shown in Fig. 9). The unimportant deviation in the Hall resistivity at high magnetic field comes from the ordinary Hall effect. These results rule out the possibility that FM originates from a magneto–optically inactive and/or insulating substance, and they strongly suggest a carrier-mediated intrinsic FM. Further study shows that the anomalous Hall conductivity is proportional to $(\sigma_{xx})^{1.6}$, with σ_{xx} represents the conductivity. This not only means that the magnitude of the AHE can be evaluated from conductivity, but also indicates the possible manipulation of AHE by external perturbations, such as field effects. Yamada *et al.*[182] for the first time demonstrated electric field-induced ferromagnetism at room temperature in oxide magnetic semiconductors by using an electric double-layer gating technique. By applying a gate voltage of a few volts, a low-carrier paramagnetic (Ti,Co)O_2 with negligible AHE was transformed into ferromagnetic state with pronounced AHE, as given in Fig. 10. This study not only supports the carrier-mediated intrinsic ferromagnetism, highlighting the crucial role of carriers played in establishing the high temperature ferromagnetism, but also offers promise that future semiconductor spintronics might operate at room temperature.

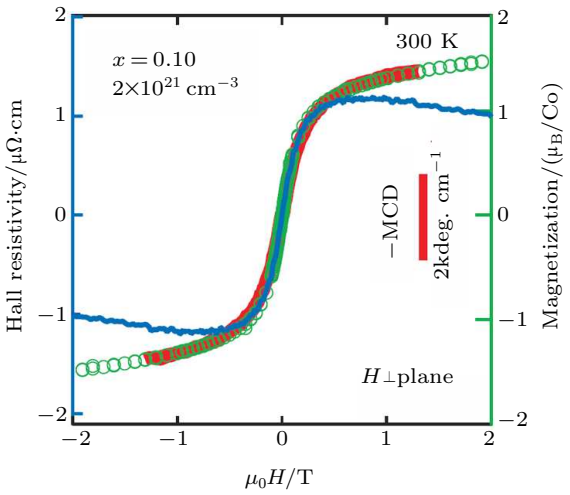


Fig. 9. Magnetic field dependence of Hall resistivity (blue curve), magnetization (green open circles), and MCD (red circles) for $Ti_{0.90}Co_{0.10}O_{2-v}$. Reprinted with permission from Ref. [113]. Copyright (2008) by IOP Publishing Ltd and Deutsche Physikalische Gesellschaft.

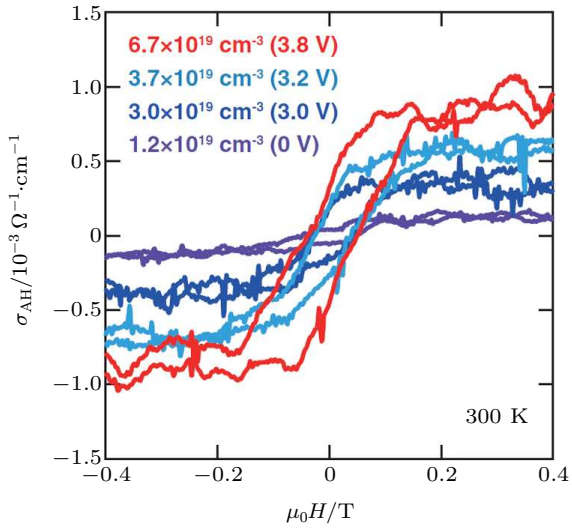


Fig. 10. (color online) Magnetic field dependence of anomalous Hall conductivity measured at 300 K under different gate voltages (V_G). Inset shows the electron density at each V_G obtained from the ordinary Hall effect. Reprinted with permission from Ref. [182]. Copyright (2011) by the American Association for the Advancement of Science.

However, AHE has also been observed in systems with secondary magnetic clusters, such as in Ni-doped ZnO[45] and Co-doped TiO_2.[47] This means that AHE itself cannot be used as an unambiguous evidence of the intrinsic FM without further detailed microscopic characterization of the studied samples.

4.3. Optical properties

Besides the spin-dependent electrical properties discussed in the previous section, strong exchange interactions

between sp carriers of host oxide semiconductors and localized d electrons of TM dopants in oxide ferromagnetic semiconductors also give rise to interesting spin-dependent optical properties. For instance, a giant Faraday effect observed in II–VI DMS $Cd_{1-x}Mn_xTe$ and $Cd_{1-x-y}Hg_yMn_xTe$ has been used for optical isolators in high-speed optical communication systems and magneto–optical waveguides for optical circuits.[184,185] Magneto–optical properties of oxide ferromagnetic semiconductors, such as TM-doped ZnO and TiO_2 etc. with a large optical band gap and high excitation binding energy, would be of particular interesting for a variety of short wavelength applications. Since ZnO is a direct band transition semiconductor, a sharp and large MCD signal should appear upon the abrupt increase in absorption. MCD and Faraday rotation as high as $2^\circ\cdot cm^{-1}\cdot Oe^{-1}$ at low temperature in $Zn_{1-x}Co_xO$ near the optical band gap has been reported by Ando *et al.*,[185,186] which are about two orders larger than those of ZnO, indicating a strong antiferromagnetic p–d exchange interaction. And the MCD signal around 2 eV corresponds to the d–d level absorption of substitutional Co^{2+} ions.[76] Moreover, a maximal Kerr rotation of 0.72° is observed at room temperature in annealed inhomogeneous $Zn_{1-x}Co_xO$ COFSs, which is even higher than that of pure Co films, Pt/Co multilayers, and Pt_xCo_{1-x} alloys.[42] While in Co-doped anatase TiO_2, a hysteresis MCD signal without any other paramagnetic signal has been reported,[187] indicating that the MCD signal originates from a single ferromagnetic source. It should be pointed out that the ferromagnetism could be extrinsic,[188] if the ambiguous relationship between the MCD and absorption spectra, the different magnetic field dependence depending on photon energy, or the superposition of several magnetic behaviors is observed.

The optical properties of oxide ferromagnetic semiconductors have also been studied by spectroscopic ellipsometry. With increasing TM doping concentrations, the optical bandgap absorption edge of the compounds shows a redshift compared to the host oxide, such as ZnO, while the transmittance spectra show an increase of both the absorption band intensity and the redshift of both the absorption peaks and the band edges. These optical studies suggest that sp–d exchange interactions and direct d–d coupling become activated with increasing TM concentrations, which results in the observed ferromagnetic properties.

5. Origin of ferromagnetism and first principles calculation of exchange interactions

Not only robust ferromagnetism has been reported in DMOSs. "Mystery" magnetic behaviors have also been observed, such as d^0 ferromagnetism and giant magnetic moments. These phenomena challenge our understanding of oxide ferromagnetism. In this section, we would like to first introduce three typical models — itinerate carrier mediated FM, bound magnetic polarons (BMPs), and charge transfer model — among the numerous models that have been proposed to explain the mechanism of observed FM, and then focus on the first principles investigations of the exchange interactions between TM dopants in DMOSs.

5.1. Origin of ferromagnetism

Carrier induced FM was first proposed by Dietl *et al.*[13] based on the Zener model. The original Zener model was later abandoned, as it considered neither the itinerant character of the magnetic electrons nor the quantum (Friedel) oscillations of the electron spin polarization around the localized spin, both of which have been established to be critical factors for the theory of magnetic metals.[189] However, we can now see that in semiconductors where the effect of quantum averages to zero because the mean distance between the carriers is greater than that between the spins, the Zener model becomes equivalent to the RKKY approach. As a result, FM above room temperature has been theoretically predicted in p-type ZnO doped with 5 at% Mn. The model of carrier-induced FM has been verified by many experiments with relatively high carrier density. In most of these systems, the FM can be enhanced by increasing the carrier density through Al codoping or introducing more oxygen vacancies and/or Zn interstitials.

In order to explain the observed FM in some insulating systems, Coey *et al.*[77] proposed that ferromagnetic exchange can be mediated by shallow donor electrons that form bound magnetic polarons (BMPs) which overlap to create a spin split impurity band. The electrons associated with particular defects remain localized in terms of hydrogenic orbits, until a critical donor concentration is reached, at which point the impurity band becomes delocalized. The donors tend to form BMPs, coupling the 3d magnetic moments of the TM dopants within their orbits. And FM occurs when $\delta > \delta_p$ and $x < x_p$, where δ_p and x_p are the polaron percolation threshold and cation percolation threshold, respectively.

The charge transfer model is developed for defect-related FM by Coey *et al.*, involving a spin-split defect band populated by charge transfers from a proximate charge reservoir.[190,191] There are three crucial components for the charge transfer FM: a defect-based band with a high density of states in the vicinity of the Fermi level; a charge reservoir to or from which electrons can be easily transferred, which is usually associated with the dopant ions in the DMOSs; an effective exchange integral associated with the defect states. Unlike a classical Stoner ferromagnet where the magnetization is uniform, a charge transfer ferromagnet is not uniformly magnetized, only the regions containing the defects become ferromagnetic.

To summarize, TM dopants are coupled ferromagnetically with each other through polarized mobile carriers in the carrier-mediated FM model, while in the BMP model, it is through localized carriers trapped by defects. Both magnetic dopants and polarized carriers contribute to the total magnetic moments in these models. In contrast, in the charge transfer model, magnetic moments are entirely localized on itinerant carriers confined in small regions, such as grain boundaries.

5.2. First-principles investigations on the exchange interactions between TM dopants in oxide-based magnetic semiconductors

Electronic structure and magnetic properties of DMOSs have been extensively studied by first-principles calculations based on the density functional theory (DFT). Reviews of general principles in diluted magnetic semiconductors[192] and the research status of particular systems, such as the ZnO-based[55,72,193] and TiO_2-based magnetic semiconductors,[72] have been published elsewhere. In this section, we focus on the contribution of first-principles calculations to the theoretical understanding of the exchange mechanism occurring in the DMOSs and discuss the improvement of theoretical approaches in recent years.

After the theoretical prediction that the Curie temperature of Mn-doped p-type ZnO is higher than room temperature based on the mean-field model,[13] much attention has been paid to the DMOSs with wide band gaps, such as ZnO, In_2O_3, and TiO_2. To eliminate the divergence of results between different theoretical methods, we just select the systematic investigations where the calculations cover a series of TM elements. Sato *et al.*[194] predicted universal ferromagnetism in TM-doped (TM:V to Ni) ZnO (except for the case of doping Mn), based on the Korringa–Kohn–Rostoker (KKR) method with the coherent potential approximation (CPA). Such results have been verified by DFT calculations within the local spin density approximation (LSDA) in a supercell approach,[195,196] indicating good consistency of the different theoretical approaches for TM-doped ZnO magnetic semiconductors. Huang *et al.* studied the electronic structure of TM-doped (TM:V to Cu) In_2O_3.[197] When two TM ions are placed close to each other (the distance between TM–TM is about 3.4 Å), the ferromagnetic ordering is found to be the lowest-energy configuration, with the only exception being Fe. The TM-doped (TM:Mn to Ni) TiO_2 systems have been calculated by the linearized muffin-tin orbital (LMTO) method. In contrast with the universal ferromagnetism in the TM-doped ZnO and TM-doped In_2O_3, only Co prefers the ferromagnetic coupling.[198,199]

It is well known that the LSDA method yields an incorrect band structure for strongly correlated magnetic systems, such as the TM oxides. For Co-doped ZnO and Co-doped TiO_2 magnetic semiconductors, the LSDA method predicts the half-metallic band structure, in contrast with the experimental observations.[196,199] Furthermore, the absence of ferromagnetism in defect-free single crystal samples suggests the antiferromagnetic coupling between Co atoms.[101,200] Such results indicate that the LSDA method may predict an incorrect spin ordering, too. The deviation of LSDA results is due to the energetically overestimated 3d orbitals of TM atoms and the underestimated band gaps of parents. The correction algorithms include the incorporation of a Hubbard U term on 3d orbitals (LSDA + U),[196,199,201,202] the implementation of self-interaction correction (SIC),[17,203,204] and the employment of a hybrid exchange–correlation functional.[205]

As shown in Fig. 11, in all cases the sign and magnitude of the interactions calculated by the LSDA + U methods are strikingly different from those obtained within the LSDA, with a suppression of ferromagnetism,[196] which is in agreement with the experimental results.[101,200] For the case of Co-doped ZnO, the LSDA + U band calculation yields a semiconducting ground state, in contrast with the half-metallic band structures obtained by the LSDA method, as shown in Fig. 12.[202]

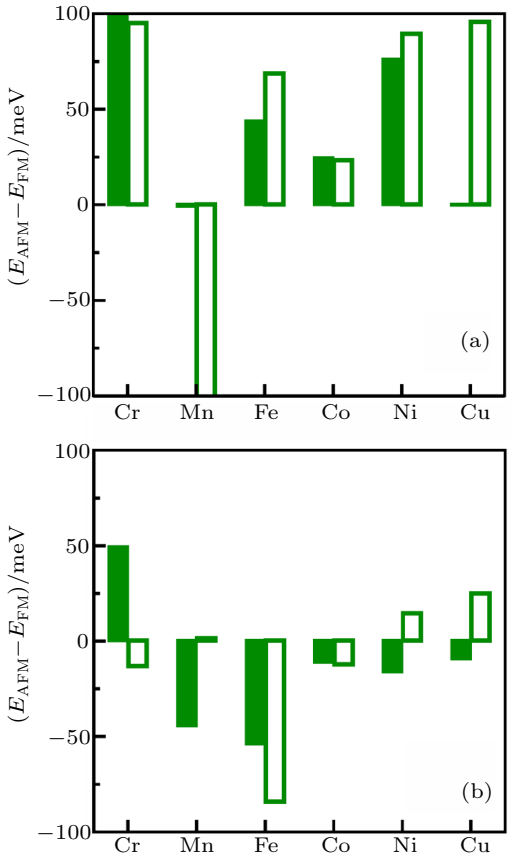


Fig. 11. LSDA energy differences ($\Delta E = E_{AFM} - E_{FM}$) for TM-doped ZnO. The filled bars represent the case when the ionic coordinates are not relaxed and the unfilled bars represent the case when the ionic coordinates are relaxed. (a) LSDA results; (b) LSDA+U results. Reprinted with permission from Ref. [196]. Copyright (2006) by the American Physical Society.

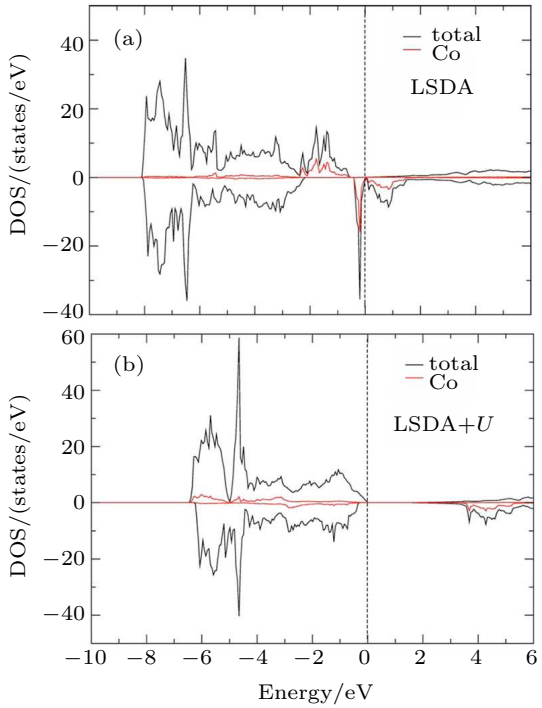


Fig. 12. DOS of Co-doped ZnO. (a) LSDA; (b) LSDA+U. Reprinted with permission from Ref. [202]. Copyright (2006) by the American Physical Society.

In the magnetic semiconductors, the exchange interactions between TM ions are closely related to the presence of weakly localized carrier.[9] To interpret the origin of ferromagnetism in Co-doped ZnO, Walsh *et al.* proposed a carrier-mediated band coupling model based on the coupling and level repulsion between the magnetic ions d and the host p states.[205,206] The anions in ZnO semiconductor form tetrahedral crystal fields, in which the 3d states of cobalt dopants split into lower e_d and upper t_{2d} states, resulting in the occupation of all the majority spin 3d states (e_d and t_{2d}) and minority spin e_d states, with a local magnetic moment close to 3 μ_B. The 3d states with the same symmetry and the same spin couple with each other through mediation of O:2p orbitals, further splitting the 3d levels: the bonding states and anti-bonding states. Since both the majority and minority e_d states are fully occupied, the splitting of e_d states yields no energy gain. Thus we shall discuss only the hybridization between Co:t_{2d} states. The exchange parameters between the majority–majority, minority–minority, majority–minority t_{2d} states are denoted as Δ^1_{dd}, Δ^2_{dd}, $\Delta^{1,2}_{dd}$, respectively. As shown in Fig. 13, the energy difference between the ferromagnetic and antiferromagnetic (AFM) spin orderings can be described as $\Delta E_{FM-AFM} = -2m_e\Delta^2_{dd} + 2[(3-m_e)\Delta^{1,2}_{dd}]$ in the case of doping Co in ZnO, where m_e is the additional number of electrons per TM^{2+} ion. The ferromagnetic interactions between occupied majority t_{2d} states results in no energy gain due to filled bonding and anti-bonding states, while AFM interactions can result in a small energy gain, in good agreement with the experimental results that no ferromagnetism is observed in defect-free samples.[101,207] On the other hand, further occupation of the minority t_{2d} states will result in a ferromagnetic ordering with lower energy as compared with the AFM one, through the energy gain from the filling of the minority bonding states. Therefore, ferromagnetic coupling can be enhanced by introducing additional n-type carriers, such as the co-doping of Al. The band structures implied in the carrier-mediated band coupling model and the carrier-enhanced ferromagnetism have been verified by first-principles calculations.[205,206] Such a model can be further extended to the exchange mechanism of Mn doped II–VI and III–V semiconductors.[206] Note that the native defects, such as the oxygen vacancies (V_O), are not required to be explicitly included in such a theoretical model. Only the n-type carriers are crucial to establish the ferromagnetic spin ordering.

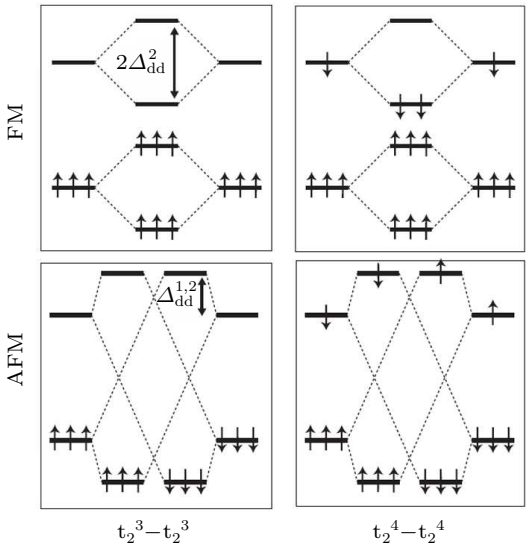


Fig. 13. Coupling of the Co:t_{2d} levels for Co_{Zn} substitution in ZnO for (left) the pure host system and (right) an n-type doped system. Reprinted with permission from Ref. [205]. Copyright (2008) by the American Physical Society.

The donor impurity states induced by the native defects, such as the oxygen vacancies, are also essential to the magnetization of oxide-based magnetic semiconductors.[77] Pemmaraju *et al.* proposed that the ferromagnetic coupling between Co–V_O pairs in ZnO can be achieved with additional n-type carriers, i.e., by a two-center model.[203] In particular, the strong long-range ferromagnetic coupling beyond the 3rd nearest-neighboring Co–V_O pairs has been predicted if a electron density of 6.7×10^{20} cm^{-3} is present. The authors claim that the Co:t_2 minority state is broadened in terms of Co–V_O and forms a t_2–V_O hybrid state right at the CBM, as shown in Fig. 14, which is very extensive in space, thus an impurity band is formed. In another DMOS parent, TiO_2, it has been reported that the presence of V_O decreases the energy required to introduce the impurities in the host lattice but increases the magnetic moment of TM ions.[198]

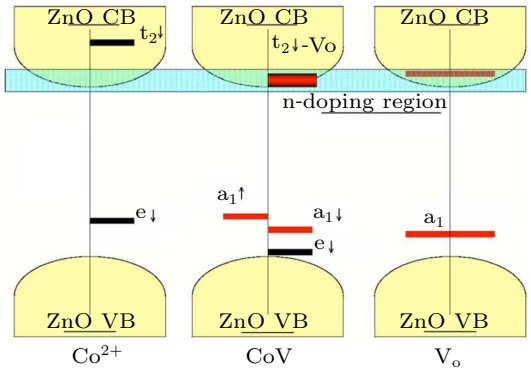


Fig. 14. Sketch of Co–V_O hybrid states (middle). Reprinted with permission from Ref. [203]. Copyright (2008) by the American Physical Society.

It is noted that in these theoretical models, the condition of high carrier concentration that pushes the Fermi level into the conduction band is explicitly required to mediate the FM exchange interactions between the Co:t_{2d} states. Actually, ferromagnetic behavior is observed in both insulating and metallic DMOSs.[92,99,208,209] To solve such a problem, Hu *et al.* recently proposed that the defect complexes can introduce the spin-polarized donor states and mediate the FM coupling, which can explain the ferromagnetism in both conductive and insulating Co:ZnO.[210]

6. Devices

The long term goal of the oxide ferromagnetic semiconductor study is to produce novel spin-based multifunctional devices, such as magnetic tunnel junctions, spin field effect transistors, and spin light emitting diodes, wherein nonvolatile information storage, high processing speed, and low energy consumption could all be achieved simultaneously. It has been proved that spin injection from a conventional ferromagnetic metal into a non-magnetic semiconductor is highly inefficient because of the fundamental conductance mismatch.[211] By using injections from Ohmic contacts or ballistic point contacts or hot electron injections, promising advances have been achieved in increasing the efficiency from metal contacts into semiconductor, but so far, reproducibility is poor. Recently, efficient spin injection has been demonstrated in all semiconductor tunnel structures.[212,213] Within this concept, making spin polarized carriers flow from oxide ferromagnetic semiconductors (TM-doepd ZnO, TM-doped TiO_2, etc.) into conventional semiconductors (ZnO, TiO_2, etc.) would be an effective way to realize high spin injection efficiency because of their good chemical and physical compatibility.

6.1. Magnetic tunnel junctions

The core structure of magnetic tunnel junctions (MTJs) consists of a thin insulating layer, which is used as a tunnel barrier, sandwiched between two ferromagnetic layers. The tunnel resistance of MTJs depends on the relative orientation of magnetic moments in two ferromagnetic layers, and the change in resistance with the parallel and antiparallel alignments of two ferromagnetic layers is known as tunneling magnetoresistance (TMR). TMR was first observed in 1975.[214] Later, large and reproducible TMR was realized based on amorphous Al_2O_3 insulating layers.[215] A further milestone in the development of TMR is the theoretical predication of over 1000% TMR in MgO-based MTJ due to the Bloch state filtering the electronic wave functions.[216,217] Soon after that, TMR exceeding 200% at room temperature was reported in MgO MTJs using Fe or CoFe ferromagnetic electrodes.[218,219] Further information can be found in several recent review papers.[220,221]

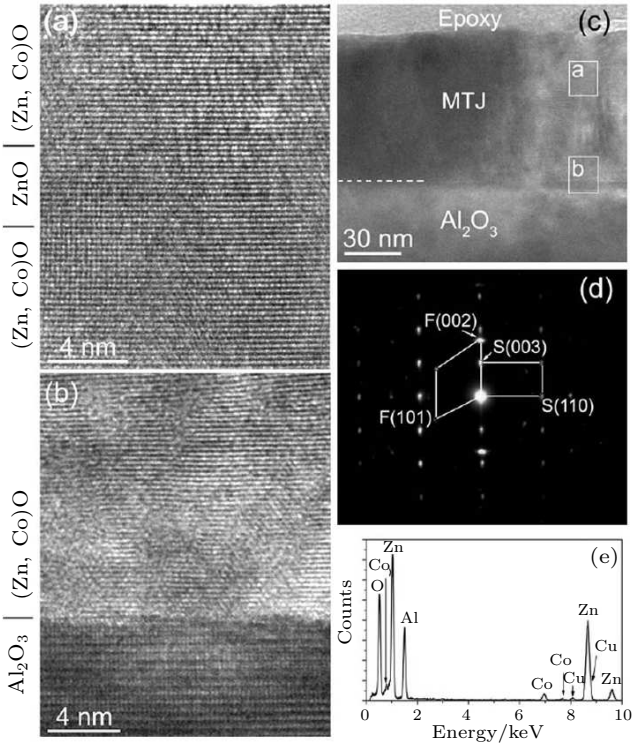


Fig. 15. (a) HRTEM image of (Zn,Co)O/ZnO/(Zn,Co)O heterostructures. (b) Cross section HRTEM of (Zn,Co)O/Al_2O_3 interface. (c) Low magnification image of MTJ cross section. (d) SAED of the MTJ, where F and S denote film and substrate, respectively. (e) The EDS from the same area presented in panel (c). Reprinted with permission from Ref. [223]. Copyright (2007) by the American Institute of Physics.

MTJs composed of oxide ferromagnetic semiconductors, such as TM-doped ZnO and TM-doped TiO_2, with Curie temperature above room temperature have drawn increasing attention for further study of spin injection and spin-polarized transport.[222–228] Song *et al.*[223] successfully synthesized fully epitaxial (Zn,Co)O/ZnO/(Zn,Co)O junctions, as shown in Fig. 15. Instead of a conventional butterfly shape, a positive TMR of 20.8% was observed at 4 K and was reduced to 0.35% at room temperature under 2-T applied field. It is believed that the observed anomalous positive TMR originates from the spin

splitting of the conduction band and a subsequent redistribution of conduction electrons when a strong s–d exchange interaction is present.[223] Also, the large energy separation between the Fermi level and the mobility edge results in anomalous voltage dependence of TMR in (Zn,Co)O-based junctions with double barriers.[224] Recently, Li *et al.* reported a negative TMR of 19.1% at 2 K in Co/ZnO/$Zn_{1-x}Co_xO$ MTJ,[227] which gave a low limit of the spin polarization ratio of 25% in the concentrated $Zn_{1-x}Co_xO$ ferromagnetic semiconductors.

TMR reflects the influence of the relative magnetization alignment between adjacent magnetic layers on the current flow. The spin-transfer torque effects represent a reciprocal interaction: a strong current can exert a torque on the magnetization of the magnetic layers and can thus influence the magnetization configuration.[229,230] There are many reports of current induced torque in layered ferromagnet–normal metal systems and layered ferromagnet–insulator systems.[231–234] To the best of our knowledge, there are no reports of spin transfer torque in oxide ferromagnetic semiconductor-based MTJs. However, great progress has been achieved in direct electrical control of magnetization in oxide magnetic semiconductors.[182,235,236] The first successful demonstration of an external electric field modulation of ferromagnetism in DMOSs was realized in a high quality epitaxial $PbZr_{0.2}Ti_{0.8}O_3$/Co:TiO_2/$SrRuO_3$ heterostructure,[236] where a strong modulation of $\sim$ 15% was achieved by switching the polarization states of $PbZr_{0.2}Ti_{0.8}O_3$. In line with this, Yamada *et al.* demonstrated electrical field-induced ferromagnetism at room temperature in Co:TiO_2 by means of electric double-layer gating with high density electron accumulation, as previously shown in Fig. 10.[182] In addition, Chen *et al.* reported that the variation of defects, such as oxygen vacancies, during the set and reset process of resistive switching results in a robust and stable variation of ferromagnetism ($\sim$ 35%) of Co:ZnO DMOSs,[235] guaranteeing an additional dimension for nonvolatile memory. With an understanding the intricate connection between magnetization and spin transport we can transform technologies that generate, store or process information via the magnetization direction, which has great promise for enhancing the functionality of semiconductor devices.

6.2. Spin field effect transistors

The concept of spin field effect transistors (FET) proposed by Datta *et al.*[237] has motivated extensive study of novel spin precision-controlled electronic devices. Huang *et al.* has demonstrated a silicon spin-FET in which spin polarized electrons are modulated by external gate voltage with 37% electron current spin polarization after transport through 10 μm of undoped single crystal silicon.[238] However, to the best of our knowledge no spin-FET based on oxide ferromagnetic semiconductors has been experimentally prepared so far. One of the major obstacles is the inability to achieve high spin injection and detection efficiency at the interfaces, because any scattering at the interfaces between the ferromagnet and the semiconductor could result in spin relaxation. An alternative is using fully epitaxial techniques during device fabrication. For instance, a ZnO-based spin-FET can be specially designed as follows to allow epitaxial growth of the device: (Zn,Co)O ferromagnetic semiconductor can be used as injector and detector and a half-metallic (Zn,Mn)O can be used as channel with an insulating ZnO as gate oxide.[55] Furthermore, to move toward reliable room temperature oxide ferromagnetic semiconductor-based spin field transistors, it is necessary to combine multiple techniques. For example, unique materials, such as half metallic oxides $La_{2/3}Sr_{1/3}MnO_3$,[239] Fe_3O_4,[240,241] and CrO_2[242,243] with $\sim$ 100% spin polarization, can be used to enhance the spin injection ratio. Novel device design could also help to fabricate transistors with low interface spin scattering.

7. Summary and outlook

To summarize, it has been demonstrated by many groups that the properties of oxide magnetic semiconductors are strongly influenced by various growth parameters, TM concentration, substrate lattice mismatch, oxygen pressure, and other factors. Various defects inside oxide magnetic semiconductors have very serious effects on its characteristics, however controlling defects, especially oxygen vacancy, is a key unresolved bottleneck, because defects are difficult to characterize experimentally and measure quantitatively. As a result, though an oxide doped with TM and/or non-magnetic elements can exhibit ferromagnetism above room temperature, there are still lots of open questions regarding the origin of the observed ferromagnetism. Multiple state-of-the-art techniques for structure characterization (XRD, AFM, TEM), chemical state analysis (XPS, MCD, XAS, etc.), and electrical transport measurement (MR, AHE) have been widely used to test whether the observed ferromagnetism is intrinsic or not. It has been demonstrated that structural defects play a crucial role for room temperature FM in these oxide ferromagnetic semiconductors regardless of the existence of free carriers. Establishing accurate correlations between defects and ferromagnetism is greatly needed and is of profound importance to understanding the origin of ferromagnetic behaviors in these systems.

Oxide magnetic semiconductors are functional metal oxides. It has been shown that their properties, such as resistivity and magnetization, can be manipulated electrically in a nonvolatile way, meaning that these magnetic oxides respond to electrical stimulation in a way that resembles a neural synapse. Therefore, promising applications may be found in new-concept multifunctional devices. For example, the

spin memristor,[244–246] wherein memresistance and magnetoresistance effect are combined, is an interesting system because multiple resistance states can be achieved by controlling electrical and magnetic parameters, presenting new possibilities toward a manyfold enhancement of data densities. Another promising new kind of magnetic sensor with ultrahigh sensitivity is the "spin battery" MTJ, in which huge tunneling magnetoresistance can be generated by the electromotive force.[247,248] It would not be surprising if oxide ferromagnetic semiconductors take a key role in future electronics, though controlling the quality of interfaces among metal oxides is an important key problem to be solved for accurate functionality modification. Hence, more efforts should be made by the community to come up with innovations in device design and system architecture that may help overcome the challenges and eventually lead to the emerging spintronics technologies.

References

[1] Zutic I, Fabian J and Das Sarma S 2004 *Rev. Mod. Phys.* **76** 323
[2] Das Sarma S 2001 *Am. Sci.* **89** 516
[3] Mauger A and Godart C 1986 *Phys. Rep.* **141** 51
[4] Treitinger L, Göbel H and Pink H 1976 *Mater. Res. Bull.* **11** 1375
[5] Steigmeier E and Harbeke G 1970 *Phys. Kondens. Mater.* **12** 1
[6] Story T, Galązka R R, Frankel R B and Wolff P A 1986 *Phys. Rev. Lett.* **56** 777
[7] Furdyna J K 1988 *J. Appl. Phys.* **64** R29
[8] Von Molnár S and Read D 2002 *J. Magn. Magn. Mater.* **242–245** 13
[9] Ohno H 1998 *Science* **281** 951
[10] Ohno H, Shen A, Matsukura F, Oiwa A, Endo A, Katsumoto S and Iye Y 1996 *Appl. Phys. Lett.* **69** 363
[11] Ohno H, Munekata H, Penney T, von Molnár S and Chang L L 1992 *Phys. Rev. Lett.* **68** 2664
[12] Macdonald A H, Schiffer P and Samarth N 2005 *Nat. Mater.* **4** 195
[13] Dietl T, Ohno H, Matsukura F, Cibert J and Ferrand D 2000 *Science* **287** 1019
[14] Tang H X, Kawakami R K, Awschalom D D and Roukes M L 2003 *Phys. Rev. Lett.* **90** 107201
[15] Jungwirth T, Niu Q and MacDonald A H 2002 *Phys. Rev. Lett.* **88** 207208
[16] Ohno Y, Young D K, Beschoten B, Matsukura F, Ohno H and Awschalom D D 1999 *Nature* **402** 790
[17] Tanaka M and Higo Y 2001 *Phys. Rev. Lett.* **87** 026602
[18] Ohno H, Chiba D, Matsukura F, Omiya T, Abe E, Dietl T, Ohno Y and Ohtani K 2000 *Nature* **408** 944
[19] Chen L, Yang X, Yang F H, Zhao J H, Misuraca J, Xiong P and Von Molnár S 2011 *Nano Lett.* **11** 2584
[20] Wang M, Campion R P, Rushforth A W, Edmonds K W, Foxon C F and Gallagher B L 2008 *Appl. Phys. Lett.* **93** 132103
[21] OlejníK K, Owen M H S, Novák V, Mašek J, Irvine A C, Wunderlich J and Jungwirth T 2008 *Phys. Rev. B* **78** 054403
[22] Burch K S, Shrekenhamer D B, Singley E J, Stephens J, Sheu B L, Kawakami R K, Schiffer P, Samarth N, Awschalom D D and Basov D N 2006 *Phys. Rev. Lett.* **97** 087208
[23] Park Y D, Hanbicki A T, Erwin S C, Hellberg C S, Sullivan J M, Mattson J E, Ambrose T F, Wilson A, Spanos G and Jonker B T 2002 *Science* **295** 651
[24] Deng J X, Tian Y F, He S M, Bai H L, Xu T S, Yan S S, Dai Y Y, Chen Y X, Liu G L and Mei L M 2009 *Appl. Phys. Lett.* **95** 062513
[25] Xiu F X, Wang Y, Zou J and Wang K L 2011 *Nano Rev.* **2** 5896
[26] Zhang S Q and Schmidt H 2010 *Materials* **3** 5054
[27] Matsumoto Y, Murakami M, Shono T, Hasegawa T, Fukumura T, Kawasaki M, Ahmet P, Chikyow T, Koshihara S and Koinuma H 2001 *Science* **291** 854
[28] Ueda K, Tabata H and Kawai T 2001 *Appl. Phys. Lett.* **79** 988
[29] Blackman M 1983 *Contemp. Phys.* **24** 319
[30] Valasek J 1921 *Phys. Rev.* **17** 475
[31] Bednorz J G and Mller K A 1986 *Z. Phys. B* **64** 189
[32] Jin S, Tiefel T H, McCormack M, Fastnacht R A, Ramesh R and Chen L H 1994 *Science* **264** 413
[33] Ramesh R and Spaldin N A 2007 *Nat. Mater.* **6** 21
[34] Zheng H, Wang J, Lofland S E, Ma Z, Mohaddes-Ardabili L, Zhao T, Salamanca-Riba L, Shinde S R, Ogale S B, Bai F, Viehland D, Jia Y, Schlom D G, Wuttig M, Roytburd A and Ramesh R 2004 *Science* **303** 661
[35] Wang Z, Hu J, Suryavanshi A P, Yum K and Yu M F 2007 *Nano Lett.* **7** 2966
[36] Kimura T, Goto T, Shintani H, Ishizaka K, Arima T and Tokura Y 2003 *Nature* **426** 55
[37] Tian Y F, Ding J F, Lin W N, David A, He M, Hu W J and Wu T 2013 *Sci. Rep.* **3** 1094
[38] King P D C and Veal T D 2011 *J. Phys.: Condens. Matter* **23** 334214
[39] Izyumskaya N, Alivov Ya and Morkoç H 2009 *Crit. Rev. Solid State Mater. Sci.* **34** 89
[40] Yan S S, Ren C, Wang X, Xin Y, Zhou Z X, Mei L M, Ren M J, Chen Y X, Liu Y H and Garmestani H 2004 *Appl. Phys. Lett.* **84** 2376
[41] Song H Q, Mei L M, Yan S S, Ma X L, Liu J P, Wang Y and Zhang Z 2006 *J. Appl. Phys.* **99** 123903
[42] Zhang Y P, Yan S S, Liu Y H, Ren M J, Fang Y, Chen Y X, Liu G L, Mei L M, Liu J P, Qiu J H, Wang S Y and Chen L Y 2006 *Appl. Phys. Lett.* **89** 042501
[43] Chambers S A 2010 *Adv. Mater.* **22** 219
[44] He M, Tian Y F, Springer D, Putra I A, Xing G Z, Chia E E M, Cheong S A and Wu T 2011 *Appl. Phys. Lett.* **99** 222511
[45] Snure M, Kumar D and Tiwari A 2009 *Appl. Phys. Lett.* **94** 012510
[46] He Y, Sharma P, Biswas K, Liu E Z, Ohtsu N, Inoue A, Inada Y, Nomura M, Tse J S, Yin S and Jiang J Z 2008 *Phys. Rev. B* **78** 155202
[47] Shinde S R, Ogale S B, Higgins J S, Zheng H, Millis A J, Kulkarni V N, Ramesh R, Greene R L and Venkatesan T 2004 *Phys. Rev. Lett.* **92** 166601
[48] Park J H, Kim M G, Jang H M, Ryu S and Kim Y M 2004 *Appl. Phys. Lett.* **84** 1338
[49] Sharma P, Gupta A, Rao K V, Owens F J, Sharma R, Ahuja R, Guillen J M O, Johansson B and Gehring G A 2003 *Nat. Mater.* **2** 673
[50] Tuan A C, Bryan J D, Pakhomov A B, Shutthanandan V, Thevuthasan S, McCready D E, Gaspar D, Engelhard M H, Rogers J W Jr, Krishnan K, Gamelin D R and Chamber S A 2004 *Phys. Rev. B* **70** 054424
[51] Song C, Geng K W, Zeng F, Wang X B, Shen Y X, Pan F, Xie Y N, Liu T, Zhou H T and Fan Z 2006 *Phys. Rev. B* **73** 024405
[52] Chang G S, Kurmaev E Z, Boukhvalov D W, Finkelstein L D, Colis S, Pedersen T M, Moewes A and Dinia A 2007 *Phys. Rev. B* **75** 195215
[53] Biegger E, Fonin M, Rdiger U, Janben N, Beyer M, Thomay T, Bratschitsch R and Dedkov Yu S 2007 *J. Appl. Phys.* **101** 073904
[54] Song C, Zeng F, Shen Y X, Geng K W, Xie Y N, Wu Z Y and Pan F 2006 *Phys. Rev. B* **73** 172412
[55] Pan F, Song C, Liu X J, Yang Y C and Zeng F 2008 *Mater. Sci. Eng. R* **62** 1
[56] Sunandana C S 1998 *Bull. Mater. Sci.* **21** 1
[57] Venkataraj S, Ohashi N, Sakaguchi I, Adachi Y, Ohgaki T, Ryoken H and Haneda H 2007 *J. Appl. Phys.* **102** 014905
[58] Alaria J, Bieber H, Colis S, Schmerber G and Dinia A 2006 *Appl. Phys. Lett.* **88** 112503
[59] Hays J, Punnoose A, Baldner R, Engelhard M H, Peloquin J and Reddy K M 2005 *Phys. Rev. B* **72** 075203
[60] Ramachandran S, Tiwari A and Narayan J 2004 *Appl. Phys. Lett.* **84** 5255
[61] Li X L, Wang Z L, Qin X F, Wu H S, Xu X H and Gehring G A 2008 *J. Appl. Phys.* **103** 023911
[62] Ando K 2006 *Science* **312** 1883
[63] Neal J R, Behan A J, Ibrahim R M, Blythe H J, Ziese M, Fox A M and Gehring G A 2006 *Phys. Rev. Lett.* **96** 197208
[64] Kobayashi M, Ishida Y, Hwang J l, Mizokawa T, Fujimori A, Mamiya K, Okamoto J, Takeda Y, Okane T, Saitoh Y, Muramatsu Y, Tanaka A, Saeki H, Tabata H and Kawai T 2005 *Phys. Rev. B* **72** 201201
[65] Wang X F, Xu J B, Cheung W Y, An J and Ke N 2007 *Appl. Phys. Lett.* **90** 212502
[66] Martínez B, Sandiumenge F, Balcells Ll, Arbiol J, Sibieude F and Monty C 2005 *Phys. Rev. B* **72** 165202

[67] Nagaosa N, Sinova J, Onoda S, MacDonald A H and Ong N P 2010 *Rev. Mod. Phys.* **82** 1539

[68] Gacic M, Jakob G, Herbort C, Adrian H, Tietze T, Brck S and Goering E 2007 *Phys. Rev. B* **75** 205206

[69] Fitzgerald C B, Venkatesan M, Dorneles L S, Gunning R, Stamenov P, Coey J M D, Stampe P A, Kennedy R J, Moreira E C and Sias U S 2006 *Phys. Rev. B* **74** 115307

[70] Philip J, Theodoropoulou N, Berera G, Moodera J S and Satpati B 2004 *Appl. Phys. Lett.* **85** 777

[71] Toyosaki H, Fukumura T, Yamada Y, Nakajima K, Chikyow T, Hasegawa T, Koinuma H and Kawasaki M 2004 *Nat. Mater.* **3** 221

[72] Janisch R, Gopal P and Spaldin N A 2005 *J. Phys.: Condens. Matter* **17** R657

[73] Pearton S J, Heo W H, Ivill M, Norton D P and Steiner T 2004 *Semicond. Sci. Technol.* **19** R59

[74] Ogale S B 2010 *Adv. Mater.* **22** 3125

[75] Prellier W, Fouchet A and Mercey B 2003 *J. Phys.: Condens. Matter* **15** R1583

[76] Jin Z W, Fukumura T, Kawasaki M, Ando K, Saito H, Sekiguchi T, Yoo Y Z, Murakami M, Matsumoto Y, Hasegawa T and Koinuma H 2001 *Appl. Phys. Lett.* **78** 3824

[77] Coey J M D, Venkatesan M and Fitzgerald C B 2005 *Nat. Mater.* **4** 173

[78] Venkatesan M, Fitzgerald C B, Lunney J G and Coey J M D 2004 *Phys. Rev. Lett.* **93** 177206

[79] Cho Y M, Choo W K, Kim H, Kim D and Ihm Y 2002 *Appl. Phys. Lett.* **80** 3358

[80] Wei X X, Song C, Geng K W, Zeng F, He B and Pan F 2006 *J. Phys.: Condens. Matter* **18** 7471

[81] Liu G L, Cao Q, Deng J X, Xing P F, Tian Y F, Chen Y X, Yan S S and Mei L M 2007 *Appl. Phys. Lett.* **90** 052504

[82] Wakano T, Fujimura N, Morinaga Y, Abe N, Ashida A and Ito T 2001 *Physica E* **10** 260

[83] Liu X, Lin F, Sun L, Cheng W, Ma X and Shi W 2006 *Appl. Phys. Lett.* **88** 062508

[84] Lee H J, Jeong S Y, Hwang J Y and Cho C R 2003 *Europhys. Lett.* **64** 797

[85] Hong N H, Sakai J, Huong N T, Poirot N and Ruyter A 2005 *Phys. Rev. B* **72** 045336

[86] Liu H, Zhang X, Li L, Wang Y X, Gao K H, Li Z Q, Zheng R K, Ringer S P, Zhang B and Zhang X X 2007 *Appl. Phys. Lett.* **91** 072511

[87] Kundaliya D C, Ogale S B, Lofland S E, Dhar S, Metting C J and Shinde S R 2004 *Nat. Mater.* **3** 709

[88] García M A, Ruiz-González M L, Quesada A, Costa-Krämer J L, Fernández J F, Khatib S J, Wennberg A, Caballero A C, Martín-González M S, Villegas M, Briones F, González-Calbet J M and Hernando A 2005 *Phys. Rev. Lett.* **94** 217206

[89] Droubay T C, Keavney D J, Kaspar T C, Heald S M, Wang C M, Johnson C A, Whitaker K M, Gamelin D R and Chambers S A 2009 *Phys. Rev. B* **79** 155203

[90] Buchholz D B, Chang R P H, Song J H and Ketterson J B 2005 *Appl. Phys. Lett.* **87** 082504

[91] Xing G Z, Yi J B, Tao J G, Liu T, Wong L M, Zhang Z, Li G P, Wang S J, Ding J, Sum T C, Huan C H A and Wu T 2008 *Adv. Mater.* **20** 3521

[92] Tian Y F, Li Y F, He M, Putra I A, Peng H Y, Yao B, Cheong S A and Wu T 2011 *Appl. Phys. Lett.* **98** 162503

[93] Herng T S, Wong M F, Qi D C, Yi J B, Kumar A, Huang A, Kartawidjaja F C, Smadici S, Abbamonte P, Sanchez-Hanke C, Shannigrahi S, Xue J M, Wang J, Feng Y P, Rusydi A, Zeng K Y and Ding J 2011 *Adv. Mater.* **23** 1635

[94] Xing G Z, Yi J B, Tao J G, Liu T, Wong L M, Zhang Z, Li G P, Wang S J, Ding J, Sun T C, Huan C H A and Wu T 2008 *Adv. Mater.* **20** 3521

[95] Schwartz D A and Gamelin D R 2004 *Adv. Mater.* **16** 2115

[96] Kittilstved K R, Norberg N S and Gamelin D R 2005 *Phys. Rev. Lett.* **94** 147209

[97] Xu X H, Blythe H J, Ziese M, Behan A J, Neal J R, Mokhtari A, Ibrahim R M, Fox A M and Gehring G A 2006 *New J. Phys.* **8** 135

[98] Venkatesan M, Stamenov P, Dorneles L S, Gunning R D, Bernoux B and Coey J M D 2007 *Appl. Phys. Lett.* **90** 242508

[99] Behan A J, Mokhtari A, Blythe H J, Score D, Xu X H, Neal J R, Fox A M and Gehring G A 2008 *Phys. Rev. Lett.* **100** 047206

[100] Kaspar T C, Droubay T, Heald S M, Engelhard M H, Nachimuthu P and Chamber S A 2008 *Phys. Rev. B* **77** 201303

[101] Ney A, Ollefs K, Ye S, Kammermeier T, Ney V, Kaspar T C, Chambers S A, Wilhelm F and Rogalev A 2008 *Phys. Rev. Lett.* **100** 157201

[102] Kaspar T C, Droubay T, Heald S M, Nachimuthu P, Wang C M, Shutthanandan V, Johnson C A, Gamelin D R and Chambers S A 2008 *New J. Phys.* **10** 055010

[103] Hong N, Prellier W, Sakai J and Ruyter A 2004 *J. Appl. Phys.* **95** 7378

[104] Stampe P, Kennedy R J, Xin Y and Parker J S 2003 *J. Appl. Phys.* **93** 7864

[105] Kim J Y, Park J H, Park B G, Noh H J, Oh S J, Yang J S, Kim D H, Bu S D, Noh T W, Lin H J, Hsieh H H and Chen C T 2003 *Phys. Rev. Lett.* **90** 017401

[106] Kennedy R J, Stampe P A, Hu E, Xiong P, Molnár S von and Xin Y 2004 *Appl. Phys. Lett.* **84** 2832

[107] Chambers S A, Thevuthasan S, Farrow R F C, Marks R F, Thiele J U, Folks L, Samant M G, Kellock A J, Ruzycki N, Ederer D L and Diebold U 2001 *Appl. Phys. Lett.* **79** 3467

[108] Yamada Y, Toyosaki H, Tsukazaki A, Fukumura T, Tamura K, Segawa Y, Nakajima K, Aoyama T, Chikyow T, Hasegawa T, Koinuma H and Kawasaki M 2004 *J. Appl. Phys.* **96** 5097

[109] Mamiya K, Koide T, Fujimori A, Tokano H, Manaka H, Tanaka A, Toyosaki H, Fukumura T and Kawasaki M 2006 *Appl. Phys. Lett.* **89** 062506

[110] Toyosaki H, Fukumura T, Yamada Y, Nakajima K, Chikyow T, Hasegawa T, Koinuma H and Kawasaki M 2004 *Nat. Mater.* **3** 221

[111] Ueno K, Fukumura T, Toyosaki H, Nakano M and Kawasaki M 2007 *Appl. Phys. Lett.* **90** 072103

[112] Toyosaki H, Fukumura, Yamada Y and Kawasaki M 2005 *Appl. Phys. Lett.* **86** 182503

[113] Fukumura T, Toyosaki H, Ueno K, Nakano M and Kawasaki M 2008 *New J. Phys.* **10** 055018

[114] Chambers S A, Heald S M and Droubay T 2003 *Phys. Rev. B* **67** 100401

[115] Shinde S R, Ogale S B, Das Sarma S, Simpson J R, Drew H D, Lofland S E, Lanci C, Buban J P, Browning N D, Kulkarni V N, Higgins J, Sharma R, Greene R L and Venkatesan T 2003 *Phys. Rev. B* **67** 115211

[116] Higgins J S, Shinde S R, Ogale S B, Venkatesan T and Greene R L 2004 *Phys. Rev. B* **69** 073201

[117] Kim Y J, Thevuthasan S, Droubay T, Lea A S, Wang C M, Shutthanandan V, Chambers S A, Sears R P, Taylor B and Sinkovic B 2004 *Appl. Phys. Lett.* **84** 3531

[118] Hong N H, Sakai J, Prellier W, Hassini A, Ruyter A and Gervais F 2004 *Phys. Rev. B* **70** 195204

[119] Kaspar T C, Heald S M, Wang C M, Bryan J D, Droubay T, Shutthanandan V, Thevuthasan S, McCready D E, Kellock A J, Gamelin D R and Chambers S A 2005 *Phys. Rev. Lett.* **95** 217203

[120] Kaspar T C, Droubay T, Shutthanandan V, Heald S M, Wang C M, McCready D E, Thevuthasan S, Bryan J D, Gamelin D R, Kellock A J, Toney M F, Hong X, Ahn C H and Chambers S A 2006 *Phys. Rev. B* **73** 155327

[121] Wang Z J, Tang J K, Zhang H G, Golub V, Spinu L and Tung L D 2004 *J. Appl. Phys.* **95** 7381

[122] Droubay T, Heald S M, Shutthanandan V, Thevuthasan S, Chambers S A and Osterwalder J 2005 *J. Appl. Phys.* **97** 046103

[123] Ogale S B, Choudhary R J, Buban J P, Lofland S E, Shinde S R, Kale S N, Kulkarni V N, Higgins J, Lanci C, Simpson J R, Browning N D, Das Sarma S, Drew H D, Greene R L and Venkatesan T 2003 *Phys. Rev. Lett.* **91** 077205

[124] Fitzgerald C B, Venkatesan M, Douvalis A P, Huber S, Coey J M D and Bakas T 2004 *J. Appl. Phys.* **95** 7390

[125] Kimura H, Fukumura T, Kawasaki M, Inaba K, Hasegawa T and Koinuma H 2002 *Appl. Phys. Lett.* **80** 94

[126] Coey J M D, Douvalis A P, Fitzgerald C B and Venkatesan M 2004 *Appl. Phys. Lett.* **84** 1332

[127] Hong N H, Buyter A, Prellier W, Sakai J and Huong N T 2005 *J. Phys.: Condens. Matter* **17** 6533

[128] Li Y F, Deng Y, Tian Y F, Yao B and Wu T 2012 *Appl. Phys. Lett.* **100** 172402

[129] Fitzgerald C B, Venkatesan M, Lunney J G, Dorneles L S and Coey J M D 2005 *Appl. Sur. Sci.* **247** 493

[130] Xing P F, Chen Y X, Yan S S, Liu G L, Mei L M and Zhang Z 2009 *J. Appl. Phys.* **106** 043909

[131] He J, Xu S, Yoo Y K, Xue Q, Lee H C, Cheng S, Xiang X D, Dionne G F and Takeuchi I 2005 *Appl. Phys. Lett.* **86** 052503

[132] Xing P F, Chen Y X, Yan S S, Liu G L, Mei L M, Wang K, Han X D and Zhang Z 2008 *Appl. Phys. Lett.* **92** 022513

[133] Raebiger H, Lany S and Zunger A 2009 *Phys. Rev. B* **79** 165202
[134] Hong N H, Sakai J, Huong N T and Brizé V 2005 *Appl. Phys. Lett.* **87** 102505
[135] Philip J, Punnoose A, Kim B I, Reddy K M, Layne S, Holmes J O, Satpati B, Leclair P R, Santos and Moodera J S 2006 *Nat. Mater.* **5** 298
[136] Panguluri R P, Kharel P, Sudakar C, Naik R, Suryanarayanan R, Naik V M, Petukhov A G, Nadgorny B and Lawes G 2009 *Phys. Rev. B* **79** 165208
[137] Xing G Z, Yi J B, Wang D D, Liao L, Yu T, Shen Z X, Huan C H A, Sum T C, Ding J and Wu T 2009 *Phys. Rev. B* **79** 174406
[138] Gupta A, Cao H, Parekh K, Rao K V, Raju A R and Waghmare U V 2007 *J. Appl. Phys.* **101** 09N513
[139] Peleckis G, Wang X L and Dou S X 2006 *Appl. Phys. Lett.* **88** 132507
[140] Guan L X, Tao J G, Xiao Z R, Zhao B C, Fan X F, Huang C H A, Kuo J L and Wang L 2009 *Phys. Rev. B* **79** 184412
[141] Kale S N, Ogale S B, Shinde S R, Sahasrabuddhe M, Kulkarni V N, Greene R L and Venkatesan T 2003 *Appl. Phys. Lett.* **82** 2100
[142] Raebiger H, Lany S and Zunger A 2007 *Phys. Rev. Lett.* **99** 167203
[143] Coey J M D 2005 *Solid State Sci.* **7** 660
[144] Venkatesan M, Fitzgerald C B and Coey J M D 2004 *Nature* **430** 630
[145] Coey J M D, Venkatesan M, Stamenov P, Fitzgerald C B and Dorneles L S 2005 *Phys. Rev. B* **72** 024450
[146] Hong N H, Sakai J, Poirot N and Brizé V 2006 *Phys. Rev. B* **73** 132404
[147] Sundaredan A, Bhargavi R, Rangarajan N, Siddesh U and Rao C N R 2006 *Phys. Rev. B* **74** 161306
[148] Xing G Z, Wang D D, Yi J B, Yang L L, Gao M, He M, Yang J H, Ding J, Sun T C and Wu T 2010 *Appl. Phys. Lett.* **96** 112511
[149] Sun S H, Wu P and Xing P F 2012 *Appl. Phys. Lett.* **101** 132417
[150] Hong N H, Poirot N and Sakai J 2007 *Phys. Rev. B* **77** 033205
[151] Pan H, Yi J B, Shen L, Wu R Q, Yang J H, Lin J Y, Feng Y P, Ding J, Van L H and Yin J H 2007 *Phys. Rev. Lett.* **99** 127201
[152] Coey J M D, Stamenov P, Gunning R D, Venkatesan M and Paul K 2010 *New J. Phys.* **12** 053025
[153] Garcia M A, Pinel E F, de la Venta J, Quesada A, Bouzas V, Fernández J F, Romero J J, González M S M and Costa-Krämer J L 2009 *J. Appl. Phys.* **105** 013925
[154] Stamenov P and Coey J M D 2006 *Rev. Sci. Instrum.* **77** 015106
[155] Quan Z Y, Xu X H, Li X L, Feng Q and Gehring G A 2010 *J. Appl. Phys.* **108** 103912
[156] Zhang Y P, Yan S S, Liu Y H, Tian Y F, Liu G L, Chen Y X, Mei L M and Liu J P 2006 *Solid State Commun.* **140** 405
[157] Tian Y F, Yan S S, Zhang Y P, Song H Q, Ji G, Liu G L, Chen Y X, Mei L M, Liu J P, Altuncevahir B and Chakka V 2006 *J. Appl. Phys.* **100** 103901
[158] Tian Y F, Zhang Y P, Yan S S, Liu G L, Chen Y X, Mei L M, Ji G and Zhang Z 2007 *Appl. Phys. Lett.* **91** 013509
[159] Tian Y F, Yan S S, Zhang Y P, Xing P F, Liu G L, Chen Y X and Mei L M 2007 *J. Phys.: Condens. Matter* **19** 326206
[160] Jin Z, Hasegawa K, Fukumura T, Yoo Y Z, Hasegawa T, Koinuma H and Kawasaki M 2001 *Physica E* **10** 256
[161] Sawicki M, Dietl T, Kossut J, Igalson J, Wojtowicz T and Plesiewicz W 1986 *Phys. Rev. Lett.* **56** 508
[162] Behan A J, Mokhtari A, Blythe H J, Ziese M, Fox A M and Gehring G A 2009 *J. Phys.: Condens. Matter* **21** 346001
[163] Hartmann L, Xu Q, Schmidt H, Hochmuth H, Lorenz M, Sturm C, Meinecke C and Grundmann M 2006 *J. Phys. D: Appl. Phys.* **39** 4920
[164] Andrearczyk T, Jaroszyński J, Grabecki G, Dietl T, Fukumura T and Kawasaki M 2005 *Phys. Rev. B* **72** 121309
[165] Xu Q, Hartmann L, Schmidt H, Hochmuth H, Lorenz M, Spemann D and Grundmann M 2007 *Phys. Rev. B* **76** 134417
[166] Xu Q, Hartmann L, Schmidt H, Hochmuth H, Lorenz M, Schmidt-Grund R, Sturm C, Spemann D, Grundmann M and Liu Y 2007 *J. Appl. Phys.* **101** 063918
[167] Peleckis G, Wang X L, Dou S X, Munroe P, Ding J and Lee B 2008 *J. Appl. Phys.* **103** 07D113
[168] Wang J, Gu Z B, Lu M H, Wu D, Yuan C S, Zhang S T, Chen Y F, Zhu S N and Zhu Y Y 2006 *Appl. Phys. Lett.* **88** 252110
[169] Dietl T, Andrearczyk T, Lipińska A, Kiecana M, Tay M and Wu Y H 2007 *Phys. Rev. B* **76** 155312
[170] Smorchkova I P, Samarth N, Kikkawa J M and Awschalom D D 1998 *Phys. Rev. B* **58** R4238
[171] Reuss F, Frank S, Kirchner C, Kling R, Gruber Th and Waag A 2005 *Appl. Phys. Lett.* **87** 112104
[172] Tian Y F, Li Y F and Wu T 2011 *Appl. Phys. Lett.* **99** 222503
[173] Matveev A K A, Glazman L I, Clarke P, Ephron D and Beasley M R 1995 *Phys. Rev. B* **52** 5289
[174] Tian Y F, Antony J, Souza R, Yan S S, Mei L M and Qiang Y 2008 *Appl. Phys. Lett.* **92** 192109
[175] Stamenov P, Venkatesan M, Dorneles L S, Maude D and Coey J M D 2006 *J. Appl. Phys.* **99** 08M124
[176] Tian Y F, Yan S S, Cao Q, Deng J X, Chen Y X, Liu G L, Mei L M and Qiang Y 2009 *Phys. Rev. B* **79** 115209
[177] Sharma N, Granville S, Kashyap S C and Ansermet J Ph 2010 *Phys. Rev. B* **82** 125211
[178] Yan S S, Liu J P, Mei L M, Tian Y F, Song H Q, Chen Y X and Liu G L 2006 *J. Phys.: Condens. Matter* **18** 10469
[179] Ye S, Ney V, Kammermeier T, Ollefs K, Zhou S, Schmidt H, Wilhelm F, Rogalev A and Ney A 2009 *Phys. Rev. B* **80** 245321
[180] Tian Y F, Lin W N and Wu T 2012 *Appl. Phys. Lett.* **100** 052408
[181] Wu D, Wei P, Johnston-Halperin E, Awschalom D D and Shi J 2008 *Phys. Rev. B* **77** 125320
[182] Yamada Y, Ueno K, Fukumura T, Yuan H T, Shimotani H, Iwasa Y, Gu L, Tsukimoto S, Ikuhara Y and Kawasaki M 2011 *Science* **332** 1065
[183] Yu Z G, He J, Xu S, Xue Q, van't Erve O M J, Jonker B T, Marcus M A, Yoo Y K, Cheng S and Xiang X D 2006 *Phys. Rev. B* **74** 165321
[184] Turner A E, Gunshor R L and Datta S 1983 *Appl. Opt.* **22** 3152
[185] Ando K, Saito H, Jin Z W, Fukumura T, Kawasaki M, Matsumoto Y and Koinuma H 2001 *J. Appl. Phys.* **89** 7284
[186] Ando K, Saito H, Jin Z W, Fukumura T, Kawasaki M, Matsumot Y and Koinuma H 2001 *Appl. Phys. Lett.* **78** 2700
[187] Fukumura T, Yamada Y, Tamura K, Nakajima K, Aoyama T, Tsukazaki A, Sumiya M, Fuke S, Segawa Y, Chikyow T, Hasegawa T, Koinuma H and Kawasaki M 2003 *Jpn. J. Appl. Phys.* **42** L105
[188] Ando K 2002 arXiv: cond-mat/0208010
[189] Zener C 1951 *Phys. Rev.* **81** 440
[190] Coey J M D, Wongsaprom K, Alaria J and Venkatesan M 2008 *J. Phys. D: Appl. Phys.* **41** 134012
[191] Coey J M D, Stamenov P, Gunning R D, Venkatesan M and Paul K 2010 *New J. Phys.* **12** 053025
[192] Sato K, Bergqvist L, Kudrnovsk J, Dederichs P H, Eriksson O, Turek I, Sanyal B, Bouzerar G, Katayama-Yoshida H, Dinh V A, Fukushima T, Kizaki H and Zeller R 2010 *Rev. Mod. Phys.* **82** 1633
[193] Liu C, Yun F and Morkoc H 2005 *J. Mater. Sci.: Mater. Electron.* **16** 555
[194] Sato K and Katayama-Yoshida H 2002 *Semicond. Sci. Technol.* **17** 367
[195] Sluiter M H F, Kawazoe Y, Sharma P, Inoue A, Raju A R, Rout C and Waghmare U V 2005 *Phys. Rev. Lett.* **94** 187204
[196] Gopal P and Spaldin N A 2006 *Phys. Rev. B* **74** 094418
[197] Huang L M, Moysés Araujo C and Ahuja R 2009 *Europhys. Lett.* **87** 27013
[198] Errico L A, Rentería M and Weissmann M 2005 *Phys. Rev. B* **72** 184425
[199] Park M S, Kwon S K and Min B I 2002 *Phys. Rev. B* **65** 161201
[200] Sati P, Deparis C, Morhain C, Schäfer S and Stepanov A 2007 *Phys. Rev. Lett.* **98** 137204
[201] Hu S J, Yan S S, Zhao M W and Mei L M 2006 *Phys. Rev. B* **73** 245205
[202] Chanier T, Sargolzaei M, Opahle I, Hayn R and Koepernik K 2006 *Phys. Rev. B* **73** 134418
[203] Pemmaraju C D, Hanafin R, Archer T, Braun H B and Sanvito S 2008 *Phys. Rev. B* **78** 054428
[204] Toyoda M, Akai H, Sato K and Katayama-Yoshida H 2006 *Physica B* **376** 647
[205] Walsh A, Da Silva J L F and Wei S 2008 *Phys. Rev. Lett.* **100** 256401
[206] Dalpian G M, Wei S, Gong X G, da Silva A J R and Fazzio A 2006 *Solid State Commun.* **138** 353
[207] Sati P, Deparis C, Morhain C, Schäfer S and Stepanov A 2007 *Phys. Rev. Lett.* **98** 137204
[208] Lu Z L, Hsu H S, Tzeng Y H, Zhang F M, Du Y W and Huang J C A 2009 *Appl. Phys. Lett.* **95** 102501
[209] Jiang F X, Xu X H, Zhang J, Fan X C, Wu H S, Alshammari M, Feng Q, Blythe H J, Score D S, Addison K, Al-Qahtani M and Gehring G A 2011 *J. Appl. Phys.* **109** 053907
[210] Hu S J, Yan S S, Zhao M W, Lin X L, Yao X X, Han C, Tian Y F, Chen Y X, Liu G L and Mei L M 2011 *Scripta Materialia* **64** 864

[211] Schmidt G, Ferrand D, Molenkamp L W, Filip A T and van Wees B J 2000 *Phys. Rev. B* **62** R4790

[212] Malajovich I, Kikkawa J M, Awschalom D D, Berry J J and Samarth N 2000 *Phys. Rev. Lett.* **84** 1015

[213] Kioseoglou G, Hanbicki A T, Sullivan J M, van't Erve O M J, Li C H, Erwin S C, Mallory R, Yasar M, Petrou A and Jonker B T 2004 *Nat. Mater.* **3** 799

[214] Julliére M 1975 *Phys. Lett. A* **54** 225

[215] Moodera J S, Kinder L R, Wong T M and Meservey R 1995 *Phys. Rev. Lett.* **74** 3273

[216] Butler W H, Zhang X G, Schulthess T C and MacLaren J M 2001 *Phys. Rev. B* **63** 054416

[217] Mathon J and Umerski A 2001 *Phys. Rev. B* **63** 220403

[218] Yuasa S, Nagahama T, Fukushima A, Suzuki Y and Ando K 2004 *Nat. Mater.* **3** 868

[219] Parkin S S P, Kaiser C, Panchula A, Rice P M, Hughes B, Samant M and Yang S H 2004 *Nat. Mater.* **3** 862

[220] Han X F, Ali S S and Liang S H 2013 *Sci. China: Phys. Mech. Astron.* **56** 29

[221] Yuasa S and Djayaprawira D D 2007 *J. Phys. D: Appl. Phys.* **40** R337

[222] Xu Q Y, Hartmann L, Zhou S Q, Mcklich A, Helm M, Biehne G, Hochmuth H, Lorenz M, Grundmann M and Schmidt H 2008 *Phys. Rev. Lett.* **101** 076601

[223] Song C, Liu X J, Zeng F and Pan F 2007 *Appl. Phys. Lett.* **91** 042106

[224] Song C, Yang Y C, Li X W, Liu X J, Zeng F and Pan F 2007 *Appl. Phys. Lett.* **91** 172109

[225] Chattopadhyay S and Nath T K 2010 *J. Appl. Phys.* **108** 083904

[226] Lee Y J, Kumar A, Marún I J V, de Jong M P and Jansen R 2010 *IEEE Trans. Magn.* **46** 1683

[227] Li Q, Shen T T, Dai Z K, Cao Y L, Yan S S, Kang S S, Dai Y Y, Chen Y X, Liu G L and Mei L M 2012 *Appl. Phys. Lett.* **101** 172405

[228] Toyosaki H, Fukumura T, Ueno K, Nakano M and Kawasaki M 2006 *J. Appl. Phys.* **99** 08M102

[229] Berger L 1996 *Phys. Rev. B* **54** 9353

[230] Slonczwski J C 1996 *J. Magn. Magn. Mater.* **159** L1

[231] Brataas A, Kent A D and Ohno H 2012 *Nat. Mater.* **11** 372

[232] Liu L, Pai C F, Li Y, Tseng H W, Ralph D C and Buhrman R A 2012 *Science* **336** 555

[233] Wang W G, Li M, Hageman S and Chien C L 2011 *Nat. Mater.* **11** 64

[234] Němec P, Rozkotová N, Trojánek F, Ranieri E De, OlejnÍk K, Zemen J, Novák V, Cukr M and Malý Jungwirth T 2012 *Nat. Phys.* **8** 411

[235] Chen G, Song C, Chen C, Gao S, Zeng F and Pan F 2012 *Adv. Mater.* **24** 3515

[236] Zhao T, Shinde S R, Ogale S B, Zheng H, Venkatesan T, Ramesh R and Sarma S Das 2005 *Phys. Rev. Lett.* **94** 126601

[237] Datta S and Das B 1990 *Appl. Phys. Lett.* **56** 665

[238] Huang B, Monsma D J and Appelbaum I 2007 *Appl. Phys. Lett.* **91** 072501

[239] Park J H, Vescovo E, Kim H J, Kwon C, Ramesh R and Venkatesan T 1998 *Nature* **392** 794

[240] Chang M T, Chou L J, Hsieh C H, Chueh Y L, Wang Z L, Murakami Y and Shindo D 2007 *Adv. Mater.* **19** 2290

[241] Liao Z, Li Y, Xu J, Zhang J, Xia K and Yu D 2006 *Nano Lett.* **6** 1087

[242] Ji Y, Strijkers G J, Yang F Y, Chien C L, Byers J M, Anguelouch A, Xiao G and Gupta A 2001 *Phys. Rev. Lett.* **86** 5585

[243] Keizer R S, Goennenwein S T B, Klapwijk T M, Miao G, Xiao G and Gupta A 2006 *Nature* **439** 825

[244] Krzysteczko P, Mnchenberger J, Schfers M, Reiss G and Thomas A 2012 *Adv. Mater.* **24** 762

[245] Hueso L E, Bergenti I, Riminucci A, Zhan Y Q and Dediu V 2007 *Adv. Mater.* **19** 2639

[246] Prezioso M, Riminucci A, Bergenti I, Graziosi P, Brune D and Dediu V A 2011 *Adv. Mater.* **23** 1371

[247] Hai P N, Ohya S, Tanaka M, Barnes S E and Maekawa S 2009 *Nature* **458** 489

[248] Miao G X, Xiao G and Gupta A 2009 *Europhys. Lett.* **87** 47006